

ECMWF Newsletter

Number 152 – Summer 2017

European Centre for Medium-Range Weather Forecasts
Europäisches Zentrum für mittelfristige Wettervorhersage
Centre européen pour les prévisions météorologiques à moyen terme

Bologna to host new data centre

IFS model and assimilation upgrade

Monitoring thin sea ice in the Arctic

Assessing the impact of observations

Calibrating precipitation forecasts

The new interpolation package MIR

© Copyright 2017

European Centre for Medium-Range Weather Forecasts, Shinfield Park, Reading, RG2 9AX, England

The content of this Newsletter is available for use under a Creative Commons Attribution-Non-Commercial-No-Derivatives-4.0-Unported Licence. See the terms at <https://creativecommons.org/licenses/by-nc-nd/4.0/>.

The information within this publication is given in good faith and considered to be true, but ECMWF accepts no liability for error or omission or for loss or damage arising from its use.

CONTENTS

EDITORIAL

A good move 1

NEWS

ECMWF supports flood disaster response in Peru 2
 New data centre to be located in Bologna 4
 New Director of Research takes up his post 4
 Ten years of forecasting atmospheric composition at ECMWF 5
 OpenIFS used by University of Reading students 6
 EFAS and GloFAS seasonal hydrological outlooks 7
 Flood forecast decision-making games 9
 ECMWF meets its users: UEF 2017 10
 Record numbers attend ECMWF's NWP courses 12
 ECMWF air quality data competition has a winner 13
 A fresh look at tropical cyclone intensity estimates 14
 ECMWF helps to upgrade Sri Lanka forecasting capability 16
 End of the road for GRIB-API 16
 New IFS version control and issue tracking tools 17

METEOROLOGY

IFS Cycle 43r3 brings model and assimilation updates 18
 Monitoring thin sea ice in the Arctic 23
 Assessing the impact of observations using
 observation-minus-forecast residuals 27
 Calibrating forecasts of heavy precipitation in river
 catchments 32

COMPUTING

The new ECMWF interpolation package MIR 36

GENERAL

ECMWF Calendar 2017/18 40
 ECMWF publications 40
 Index of Newsletter articles 41
 Contact information 43

PUBLICATION POLICY

The *ECMWF Newsletter* is published quarterly. Its purpose is to make users of ECMWF products, collaborators with ECMWF and the wider meteorological community aware of new developments at ECMWF and the use that can be made of ECMWF products. Most articles are prepared by staff at ECMWF, but articles are also welcome from people working elsewhere, especially those from Member States and Co-operating States. The *ECMWF Newsletter* is not peer-reviewed.

Editor: Georg Lentze

Typesetting and Graphics: Anabel Bowen with the assistance of Simon Witter

Cover image: Hurricane Patricia off the coast of Mexico on 23 October 2015 (*Copyright: 2015 EUMETSAT*)

Any queries about the content or distribution of the *ECMWF Newsletter* should be sent to Georg.Lentze@ecmwf.int

Guidance about submitting an article is available at www.ecmwf.int/en/about/news-centre/media-resources

CONTACTING ECMWF

Shinfield Park, Reading, Berkshire RG2 9AX, UK

Fax: +44 118 986 9450

Telephone: National 0118 949 9000

International +44 118 949 9000

ECMWF website: www.ecmwf.int

A good move

On 22 June ECMWF's Council approved the Italian city of Bologna as the location of ECMWF's new data centre. This is a vitally important decision: the Centre's premises in Reading are unable to support the growth in computing power on which continued progress in numerical weather prediction (NWP) depends. To understand this dependence, we need to remember that the skill of global weather forecasts which we take for granted today has been hard won. It is the result of many incremental improvements: in the number and quality of Earth system observations; in data assimilation; in Earth system modelling and ensemble methods; and in the resolution at which we can analyse and predict the state of the atmosphere and related parts of the Earth system.

These improvements have been made possible by scientific advances, of course, but also by sustained growth in computational capacity and substantial efficiency gains. To extend the range of skilful ensemble forecasts further, as our ten-year Strategy demands, progress needs to be made on all these fronts. The upgrade of our Integrated Forecasting System (IFS) described in this Newsletter is a case in point. It brings improvements both in modelling and in the number and use of observations, notably leading to better predictions of tropical cyclones. But it also includes changes in software infrastructure which increase efficiency and prepare the ground for future improvements.

ECMWF's new interpolation package MIR presented in this Newsletter is another illustration of how NWP research and software as well as hardware development must go hand in hand. MIR has been developed in response to the introduction of different NWP grids and parameters over the years as well as the development of new software and hardware technologies. Its flexible design and links to the IFS's Atlas library ensure that software and operational services will be able to react fast to new research developments.

Meanwhile, the results of monitoring thin sea ice in the Arctic presented in this Newsletter illustrate the way in which a growing number of satellite observations can feed into better Earth system modelling for NWP. A new sea-ice thickness product provided by the University of Hamburg, based on satellite observations from the European Space Agency's SMOS mission, is helping to evaluate the performance of ECMWF's OCEAN5 ocean/sea-ice model implemented last year.

A final remark on Bologna: the data centre decision was the subject of the first ever tweet posted by the Centre on its official Twitter account. While we have had a corporate presence on LinkedIn for some time, using Twitter and Facebook marks a new departure for the Centre. Our plan is to use those platforms to better share our science with users and partners around the world. ECMWF will begin to use these channels regularly from September.

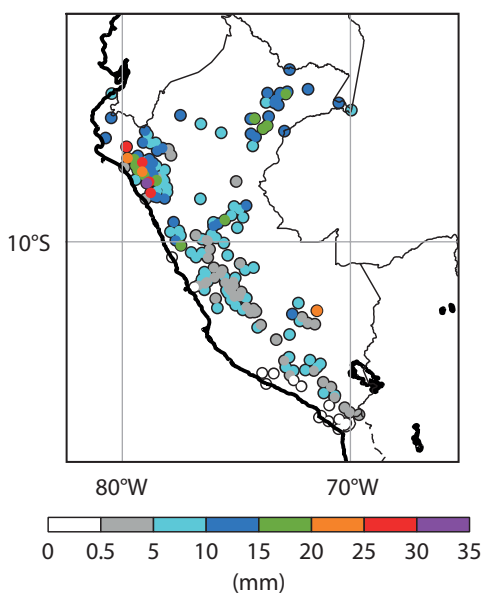
Florence Rabier

Director-General

ECMWF supports flood disaster response in Peru

FATIMA PILLOSU, UMBERTO MODIGLIANI, LINUS MAGNUSSON (all ECMWF), **MARTI BONSHOMS CALVELO** (SENAMHI, Peru), **LUISA STERPONI** (consultant for Peruvian Defence Ministry), **MARIA-HELENA RAMOS** (Irstea, France), **PATRICIO VALDERRAMA** (COEN, Peru)

From March 2017, ECMWF provided Peru with its forecast products for a limited period of time to help the country deal with the exceptionally heavy rainfall it experienced in the first few months of the year. As early as 3 February, the government declared a state of emergency in all coastal regions. The most affected areas were in the north (Tumbes, Lambayeque and Piura). In Piura, several records for daily precipitation were broken: on 3 March in El Partidor, 258.5 mm was recorded; 121.6 mm was measured on 21 March in San Miguel; and between February and March in the area of Morropon 150 mm was exceeded on three occasions. In this area, in the past similar amounts have only been recorded during exceptional El Niño events, such as those seen in 1983 and 1998.



Precipitation observations. Average daily precipitation during March 2017 according to observations received from SENAMHI.

The rainfall led to rising waters in coastal ravines. In more southern mountainous regions, this led to what is known in Peru as 'huaicos', which are a mixture of water, mud and rocks. Several rivers burst their banks causing flooding and damage to housing and infrastructure in urban and rural areas; the failure of drainage systems; and disruption of the electricity supply and sewage treatment plants. As of 31 March, the disaster had left 101 people dead, 353 injured and 19 missing, while more than 200,000 homes had been destroyed or had become uninhabitable (figures from COEN, Centro Operaciones de Emergencia Nacional of the Peruvian Ministry of Defence).

Seasonal forecast

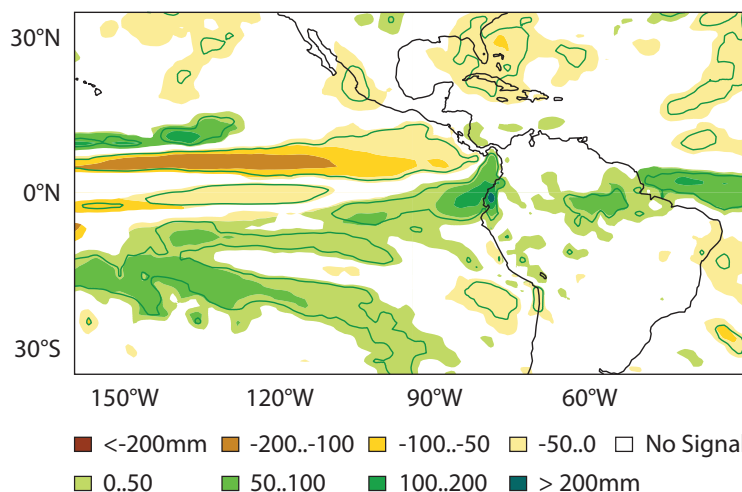
This anomalous rainfall is believed to be connected to warm sea-surface temperatures along the coast (a phenomenon called El Niño Costero), which were probably caused by an equatorial Kelvin wave in the ocean. This feature propagated from the Western Pacific, where it was first observed in the autumn of 2016 as a positive sea-surface height anomaly. Probably as a result of capturing the Kelvin wave early on, ECMWF's seasonal forecast was able to predict the anomalous rainfall along the equatorial coast of South America. The forecast from 1 November 2016 showed a wet anomaly over the region

in the February to April average.

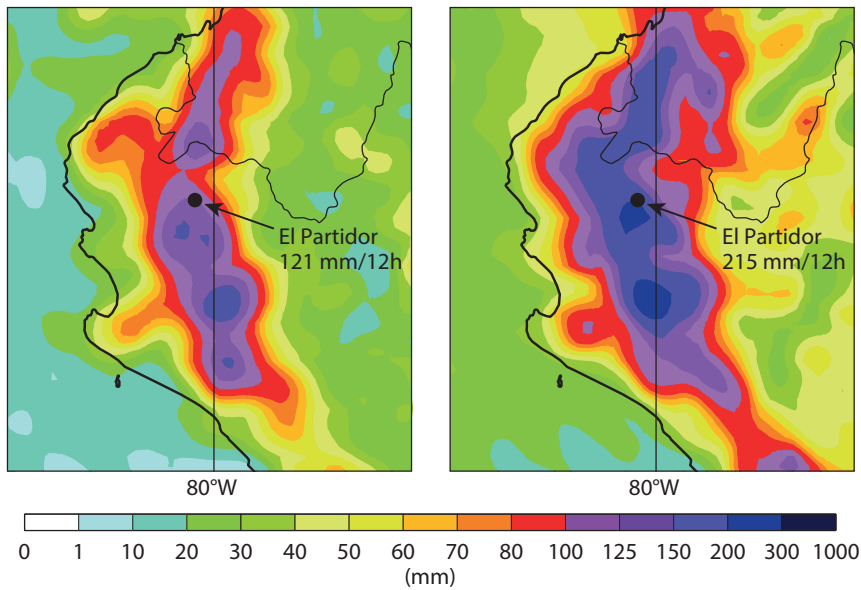
ECMWF's response

On 26 March, ECMWF received a request for rainfall forecasts from the environmental expert deployed from France (Institut national de recherche en sciences et technologies pour l'environnement et l'agriculture, Irstea) to Peru by the European Union Civil Protection Mechanism (EUCPM) through the European Civil Protection and Humanitarian Aid Operations (ECHO). Due to the exceptional circumstances, ECMWF agreed to provide its forecast products to the Peruvian Meteorological and Hydrological Service (SENAMHI) and COEN for a limited period of time, in accordance with our rules for the distribution of real-time data.

Access to all web products and ecCharts was granted and experts with previous knowledge of ECMWF products facilitated the uptake by local services. ECMWF established technical contacts with staff at SENAMHI and provided access to binary data in GRIB format in order to allow local services to process the information through their visualisation and impact models. Access to a new test product, Point-Rainfall, was also granted. It consists in statistical post-processing of ECMWF ensemble forecasts (ENS) to produce probabilistic rainfall forecasts for points. The idea is to provide better guidance in cases of localised extreme rainfall.



Seasonal forecast. Ensemble mean anomalies for precipitation in the period February–April 2017 in the ECMWF seasonal forecast from 1 November 2016.



Probabilistic rainfall forecasts for points. El Partidor in the Piura region saw 258 mm of rain on 3 March 2017, most of which fell between 4 p.m. and 10 p.m. local time. The charts relate to ECMWF forecasts of 12-hour precipitation issued on 27 February 2017 at 00 UTC (t+114 to t+126). They represent the 98th percentile for total precipitation from the raw ensemble forecast (left) and from the Point-Rainfall product (right). The risk area for heavy rainfall was well identified in both forecasts even five days in advance, but the raw ensemble did not suggest the possibility of the observed amount of 258 mm. The Point-Rainfall product, on the other hand, suggested that there was a chance, albeit a small one, of such an event occurring.

Use of ECMWF products

ECMWF web products helped SENAMHI forecasters to issue warnings of heavy rainfall that was likely to cause new flooding or to exacerbate existing flooding. Special attention was also paid to events that could hinder rescue operations and/or endanger rescuers' lives.

The binary data was used to produce extreme precipitation forecast maps. The daily total precipitation forecast from ECMWF's high-resolution forecasts (HRES) was combined with percentile maps generated from SENAMHI's climatological and hydrological

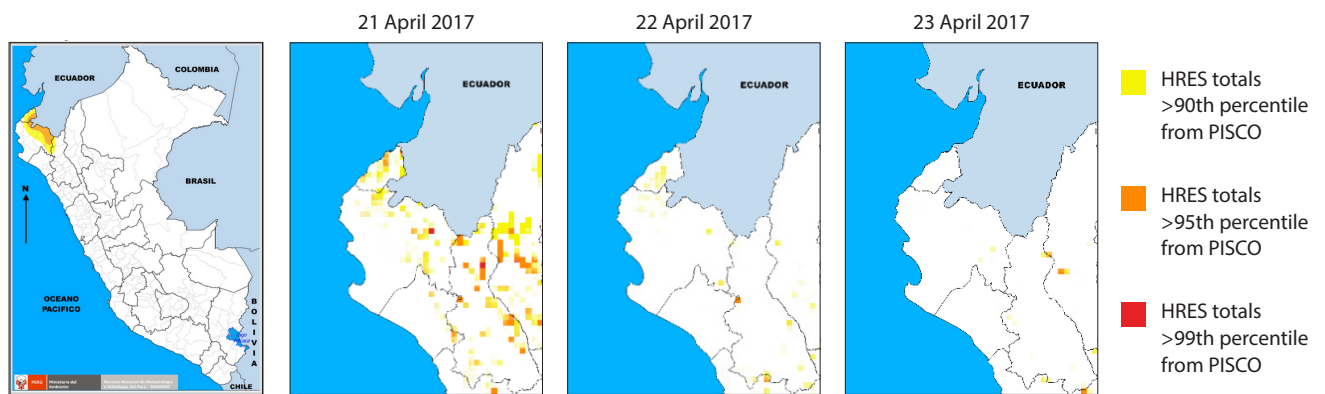
observations (PISCO), which is a gridded database for daily precipitation. The percentile maps showed the areas where the daily accumulated total precipitation (from 12 to 12 UTC) exceeded the 90th, 95th and 99th percentiles of the local climatology. This made it possible to highlight the areas facing a high risk of heavy rainfall and thus to issue corresponding warnings to COEN, the authorities, members of the Peru Disaster Risk Management System, the media and public users.

At the same time, ECMWF products were also used by the scientific team at COEN, who monitored the emergencies



Weather warning. Example of a meteorological warning map issued by SENAMHI covering the period from 3 to 9 March 2017. The risk levels range from 'one' (no special precautions necessary – white) to 'four' (be extremely cautious – red).

triggered by the precipitation and issued alert reports every three hours. ECMWF products were used alongside satellite images and local reports to enhance the accuracy of daily local rainfall forecasts and to enable better warnings of extreme rainfall and river floods. The use of forecast products by emergency teams in the field and during the early recovery phase not only improved preparedness for high-impact events but also helped to devise better-informed response plans. The cooperation with ECMWF has led SENAMHI to evaluate the possibility of acquiring a full NMHS (national meteorological and hydrological service) non-commercial licence to continue to have access to the full range of ECMWF forecast products.



High-resolution forecasts. Meteorological warning map and Categorized Rain Maps (CRM) issued for the warning from 21 to 23 April 2017, using ECMWF HRES (forecast issued on 18 April 2017 at 12 UTC). These charts do not cover days on which the rainfall was at its heaviest. The heaviest rainfall occurred in March, but SENAMHI did not have access to ECMWF data for those days.

New data centre to be located in Bologna

ECMWF Member States have approved the proposal by the Italian Government and the Emilia Romagna Region to host ECMWF's new data centre in Bologna. The decision was taken on 22 June at the end of a two-day session of Council, the Centre's governing body, which includes representatives of all its Member States. The building is to be delivered

to ECMWF by 2019 and will host the Centre's new supercomputers, whilst the Centre's headquarters are to remain in the UK.

The Italian proposal to host the data centre had been evaluated as part of an international competition and was judged at the beginning of the year to best meet ECMWF's requirements. Member States then tasked Director-

General Florence Rabier with entering into discussions with the Italian Government with a view to having a high-level agreement ready for this Council session.

Dr Rabier said she was delighted with the outcome. *"This new facility will allow us to upgrade our high-performance computing capability to the levels required to continue to advance weather science,"* she said. *"We are extremely grateful to all our Member States, who have taken great care to ensure that ECMWF's best interests would prevail."* Council President Professor Miguel Miranda added that *"today's decision will enable the Centre to start planning in earnest for the procurement of its next supercomputing system. On behalf of our Council of Member States, I want to join the Director-General in expressing our gratitude to all Member States, who have participated actively in this process."* Italian Minister of Environment Gian Luca Galletti said the decision was *"a great success for Italy"* and *"a responsibility that Bologna will surely honour."*

For further details on the decision, visit: www.ecmwf.int/en/about/media-centre/press-kit-bologna-host-ecmwfs-new-data-centre.



Council session. The Head of the Italian National Meteorological Service, Col. Silvio Cau, and ECMWF Director-General Florence Rabier (seated) signed the high-level agreement on the data centre in the presence of representatives from all 22 ECMWF Member States.

New Director of Research takes up his post

Andrew Brown took up his position as ECMWF's Director of Research on 1 July. His appointment had been approved by ECMWF's Council in December 2016. He was previously the Director of Science at the UK Met Office.

"After a couple of visits to ensure a smooth transition, I am delighted to have officially started in my new role," Dr Brown said. *"One of my first tasks will be to get to know people both in the Research Department and in the other departments with which Research works in order to help deliver ECMWF's Strategy. The Strategy sets ambitious goals for the next eight*

years. Meeting them will require a sustained research effort across all areas of numerical weather prediction. Collaboration of our hugely skilled staff with scientists in our Member and Co-operating States and beyond will be a key to success."

Dr Brown succeeds Erland Källén, who stepped down from the post after eight years to resume his professorship in dynamic meteorology at Stockholm University. A symposium held at the Centre on 8 June to mark Professor Källén's departure brought together leading World Meteorological Organization officials and experts in

numerical weather prediction (NWP). For details on the event, visit: www.ecmwf.int/en/about/media-centre/news/2017/top-nwp-experts-mark-research-directors-departure.



Andrew Brown. Dr Brown officially started at the Centre on 1 July.

Ten years of forecasting atmospheric composition at ECMWF

JOHANNES FLEMMING,
VINCENT-HENRI PEUCH,
LUKE JONES

On 17 May 2007, the first graphs showing daily forecasts of reactive gases such as carbon monoxide and tropospheric ozone were published on the ECMWF website. This marked the beginning of daily atmospheric composition forecasting at ECMWF, which is now run operationally by the EU-funded Copernicus Atmosphere Monitoring Service (CAMS) operated by the Centre.

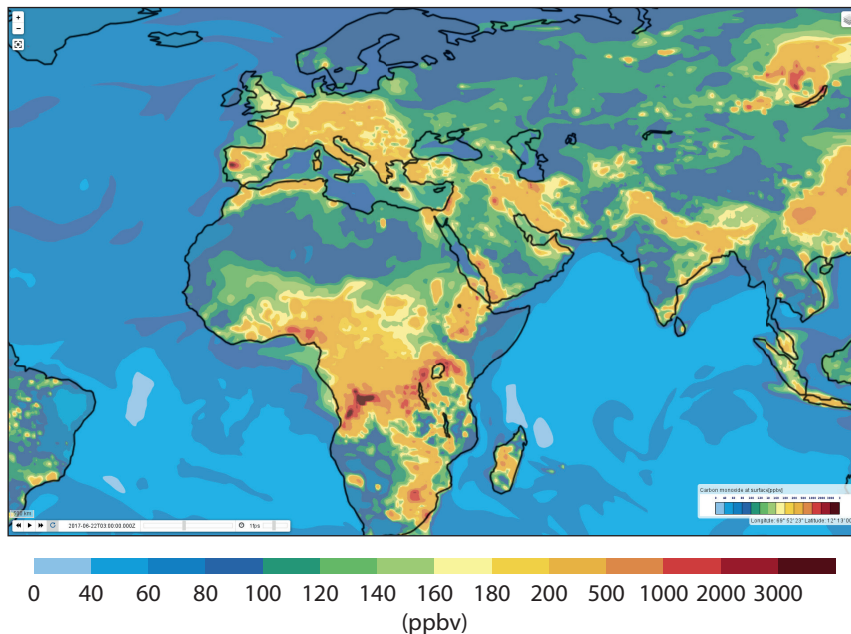
Initiated by the late Tony Hollingsworth, the GEMS project started in 2005 to build the capacity for a regional and global forecasting and data assimilation system of atmospheric composition. The idea for the global component of the GEMS system was to extend ECMWF's Integrated Forecasting System (IFS) in such a way that it could also be used for data assimilation and modelling of atmospheric composition in the troposphere and stratosphere.

First steps

A noteworthy aspect of atmospheric composition developments at ECMWF is that they have been carried out in close collaboration with European partners, such as the Dutch national meteorological service (KNMI), the French national meteorological service (Météo-France), the National Center for Scientific Research (CNRS) in France and the Forschungszentrum Jülich in Germany.

First building blocks for the assimilation of stratospheric ozone were already in place before GEMS. They were further developed for the assimilation of reactive gases, aerosols and greenhouse gases. The inclusion of modelling components to simulate emissions injection, deposition and chemical conversion started as a collaborative effort in the GEMS project, was pursued in the series of MACC projects and is now continued in CAMS.

In 2005, directly including a complex atmospheric chemistry mechanism



Carbon monoxide forecast. Carbon monoxide (CO) at the surface on 22 June 2017 as predicted by the global CAMS system using the IFS. The map was generated using the interactive plotting tools available at <http://atmosphere.copernicus.eu/maps>. Intensive forest fires in Portugal caused increased emissions of CO and other air pollutants in Europe at that time.

consisting of 50–100 tracers and 200–400 chemical reactions in the IFS was regarded as an uncertain venture. Instead a coupled approach was suggested: by means of the OASIS 4 coupler, three global chemical transport models (MOZART 3.5, MOCAGE and TM5) were coupled to the IFS. In the coupled system, the IFS would only transport and assimilate five key chemical species (CO, NO_x, SO₂, CH₂O and O₃), while the modelled source and sink terms were provided by the coupled chemical transport model. The first forecasts in May 2007 were generated by the coupled system IFS-MOZART without the assimilation of atmospheric composition observations.

A major step in the development of the CAMS global system was the introduction of data assimilation of aerosol optical depth and selected reactive gases in operational forecasts in July 2008. Other important upgrades of the system include improvements in the prediction of ozone hole chemistry

and the use of daily observed biomass burning emissions (GFAS).

Towards an integrated system

The coupled system was finally retired in September 2014 because of its low computational efficiency. Following the example of aerosols, a chemistry scheme (CB05) had been integrated into the IFS within the MACC projects. The computational efficiency of the integration into the IFS finally enabled an upgrade in the horizontal resolution of the CAMS forecasting system from T255 (80 km) to T511 (40 km) in June 2016. Still, including chemistry and aerosols in the IFS increases the computational cost of a forecast by a factor of five, and that of a complete data assimilation cycle by a factor of two.

CAMS composition forecasts are run in the operational environment used for numerical weather prediction. After including new atmospheric composition developments in the latest IFS cycle, a preparatory system (e-suite) is run to evaluate forecast performance. The e-suite is later turned

into the operational CAMS forecast suite (o-suite). Composition forecasts initialised only from the previous forecasts without data assimilation, as they were run ten years ago, are still run in research mode. They have proven to be very useful to evaluate the impact of the assimilation of atmospheric composition observations on forecast results.

CAMS global operational products have many uses, starting from the CAMS ensemble of regional air quality models in Europe, which use the global forecast as boundary conditions. The global CAMS system predicts dust storms and aerosols or plumes of air pollutants from wildfires. As part of the European

project PANDA, CAMS global forecasts have demonstrated significant skill for air quality forecasting over China. Ozone and aerosol prediction are used to underpin the CAMS UV forecast and to assess the solar power potential for the energy sector. Several scientific aircraft campaigns to measure air pollution have used specially tailored CAMS composition forecasts to assist in the flight planning.

A planned upgrade of the CAMS global forecast suite will see an increase of the vertical resolution to the 137 level configuration of ECMWF's operational weather forecasts. A high-resolution (9 km) forecast of the greenhouse gases CO₂

and methane will also be added to the CAMS product portfolio. Other upgrades in the pipeline include more advanced options to represent chemical and aerosol processes to improve the model components of the IFS. Another important development effort will be to enable the assimilation system to correct surface emissions. The assimilation of new atmospheric composition observations from the Copernicus space component, such as the polar-orbiting Sentinel 5P (later Sentinel 5) and the geostationary Sentinel 4 satellites, will bring opportunities to further improve atmospheric composition analyses and forecasts at ECMWF.

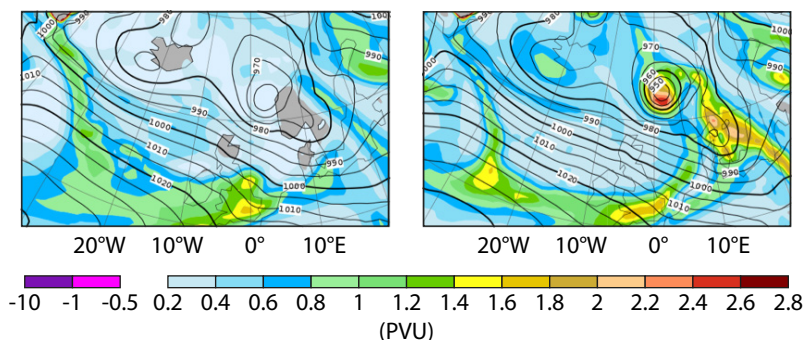
OpenIFS used by University of Reading students

ROBERT PLANT, SUZANNE GRAY (both University of Reading)

The OpenIFS programme has allowed the Integrated Forecasting System (IFS) to be made available to external institutes for both research and teaching purposes. At the University of Reading we have been experimenting with its use as a teaching tool for Masters-level students and have been encouraged by the enthusiasm of and benefits for students. It has worked particularly well for intensive small-team projects. We intend to continue developing and innovating our teaching using the model, and to expand its use. Here we describe some of our experiences with OpenIFS, with a focus on the team project.

Team projects

For one week in February, our Masters students take a break from their normal classes and collaborate in groups of three or four to delve into a research topic. One aim is to build up some confidence and experience in advance of summer dissertation work on individual projects, but the week also supports the development of team-working skills and provides a chance to try something new and different from the rest of the syllabus. We offered two OpenIFS team projects in 2016 and again in 2017 and were oversubscribed, with 11 of the 34 students naming these as their first choice this year.



Storm Nina simulations. Mean sea-level pressure (contours) and 700-hPa potential vorticity (shading) for simulations of storm Nina with 10% of the default latent heating (left) and double the default latent heating (right). Both plots are at the time of the peak intensity of the storm.

This year, each project focussed on a case study of an intense extratropical cyclone: one on storm Nina, a 'bomb' event from 10 January 2015, and the other on storm Gertrude, which produced strong winds along the Scandinavian coast on 29 January 2016. On the Monday morning, all of the students were supported to run a two-day control simulation for their case, and to view and explore their own output using Metview. We wanted to find a good balance between students experiencing the process of running a numerical weather forecast and not overburdening them with a long process of Unix environment configuration and technical instruction. In 2016, we perhaps did make the process over-technical and some students were not fully up and running until the end of the day. A more judicious use of scripting

this year enabled everyone to get started quickly and kept the enthusiasm high. All of the students gained a good sense of achievement from the hands-on use of a complex forecasting model, a type of model that they had previously only learnt about in traditional lecture settings.

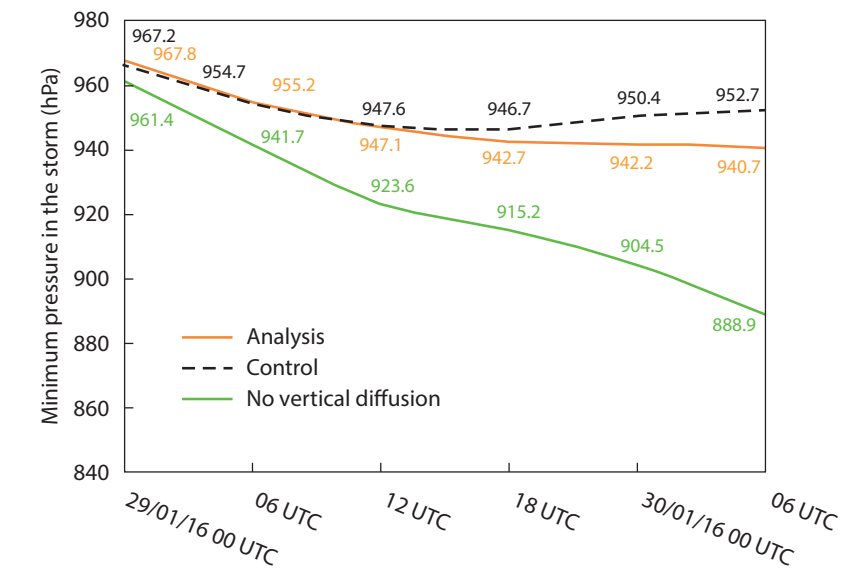
For the remainder of the week, the students assessed the meteorology of their case, making use of the simulation results and any literature and observations that they could find. There was a daily meeting with the supervisor to review progress and share ideas and, at the end of the week, each team co-wrote a report and gave a 20-minute presentation of the findings to their peers. The teams were required to devise, perform and assess further experiments with the OpenIFS to deepen their understanding.

This year, the group studying storm Nina hypothesised that latent heat release was an important factor in its explosive development and tested this by setting larger or smaller values for the latent heat of vaporisation. The group studying Gertrude focussed on the effects of boundary-layer friction on the strong near-surface winds: in one experiment they switched off the vertical diffusion entirely and thereby convincingly demonstrated to themselves that friction is an important control on storm development.

Student comments this year included: *"I really enjoyed using OpenIFS in the Team Project. I've gained skills other than in reading and evaluating research, and personally it's something I would be keen to use in the future, if there's an opportunity to do so. Seems like there's a lot of scope with the model!"* and: *"Personally, I really valued our chance to use OpenIFS, especially as my goal is for a career in forecasting."*

Growing use

Some students have also been keen to use OpenIFS for dissertation projects, and there are three such projects ongoing this summer, following on from one each in summer 2015 and 2016. Two of the three students who chose dissertation projects using OpenIFS this summer are among the eight students who



Evolution of Storm Gertrude. Time series of the mean sea-level pressure at the centre of storm Gertrude from 00 UTC 29 January to 06 UTC 30 January 2016 in the analysis (black dashed line), as simulated by the control configuration of the model (orange line; t+12 to t+42) and in a simulation without vertical diffusion (green line).

used it in their team project. The positive responses from students are encouraging us to keep expanding the use of OpenIFS, and there is increasing interest amongst the other academics to do so as well. For the year 2017/18, there are plans to introduce hands-on modelling for many more of our students by incorporating some OpenIFS work within an MSc module on Forecasting Systems and even within

a final-year undergraduate module on Numerical Weather Prediction.

We are very grateful for the invaluable support and advice of Glenn Carver (ECMWF) in the use of OpenIFS, Maria Broadbridge (Reading) for installation of the model on our local Unix cluster and technical support for its use, and Sandor Kertesz (ECMWF) for the Metview plotting scripts used by the students.

EFAS and GloFAS seasonal hydrological outlooks

LOUISE ARNAL, REBECCA EMERTON, FREDRIK WETTERHALL, CHRISTEL PRUDHOMME, PAUL SMITH, ERVIN ZSOTER, FLORIAN PAPPENBERGER (all ECMWF), **HANNAH CLOKE, LIZ STEPHENS** (both University of Reading)

One key theme of ECMWF's four-year plan is to design new forecast products that can be used operationally. The Environmental Forecast team is contributing to this theme through the extension of EFAS and GloFAS (the European and Global Flood Awareness Systems) to cover sub-seasonal to seasonal timescales.

Both the EFAS and GloFAS seasonal

outlooks are produced by forcing the Lisflood hydrological model with ECMWF's System 4 seasonal meteorological forecasts, although the methodology differs slightly between the two systems. EFAS uses the land surface and routing components of Lisflood for the European river network, while GloFAS uses the surface and sub-surface runoff from the HTESSEL land surface scheme within the IFS, and it uses Lisflood to route this through the global river network. The products both show weekly, basin-averaged river flow forecasts indicating whether major rivers are likely to be unusually dry or wet, out to two months (EFAS) and four months (GloFAS). While the skill of these seasonal outlook products has not yet been fully evaluated, they have

the potential to give earlier warnings of floods and droughts, for increased preparedness and disaster risk reduction.

The EFAS seasonal outlook

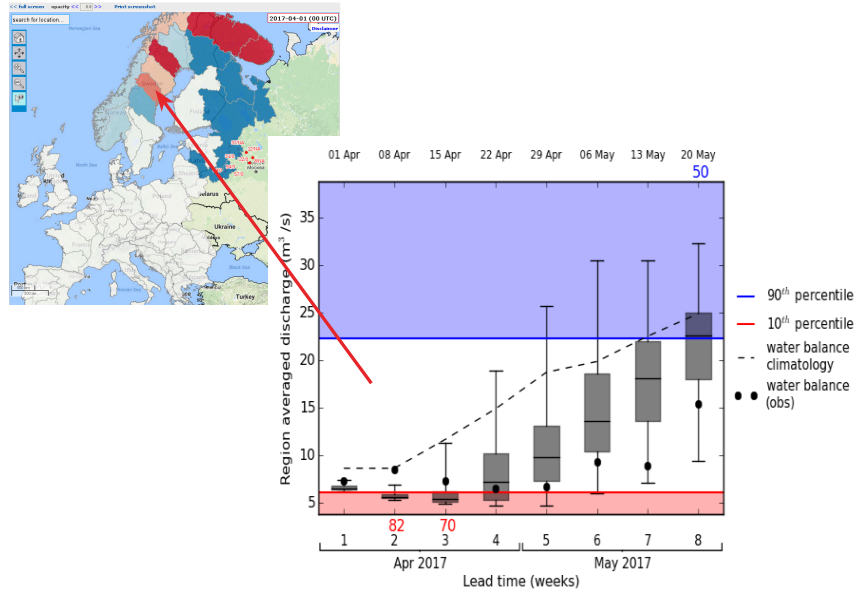
The EFAS seasonal outlook became operational in December 2016. It is one of the first operational pan-European seasonal hydrological products. This new web product shows the predicted river flow anomaly and its probability of occurrence for the next eight weeks for 74 river basins across Europe. Each basin can be clicked on to call up a hydrograph showing the ensemble river flow forecast, relevant climatological thresholds and the current pseudo-observed river flow (EFAS meteorological observations run

through Lisflood), once available. The EFAS seasonal outlook was able to capture the drought in Sweden that started last winter. The chart shows the low flow forecast (the forecast is below the climatological median for the entire forecast horizon) for April–May 2017, the start of the spring flood season in Sweden. This is due to unusually low precipitation across much of Sweden in the autumn and winter of 2016, leading to low levels in lakes, rivers and aquifers throughout the country. An early indication of droughts is invaluable for reservoir managers and hydropower generation. Although the EFAS seasonal outlook is already operational on the www.efas.eu website, we are in the process of improving and updating the product. If you have any suggestions or would like more information, please contact louise.arnal@ecmwf.int.

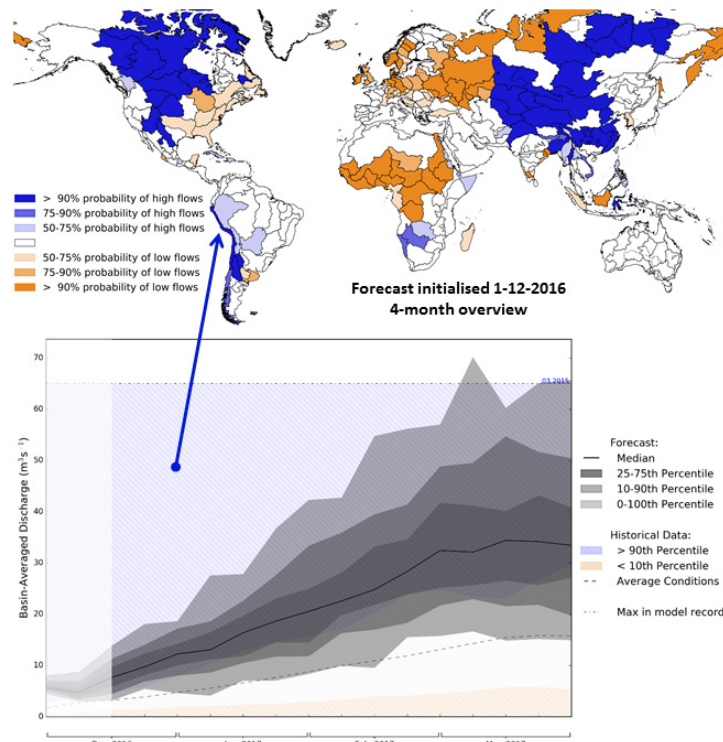
The GloFAS seasonal outlook

GloFAS-Seasonal is in the pre-operational phase. In autumn 2017 it will become an operational global-scale seasonal hydrological outlook. The GloFAS interface will show an overview map of the forecast for 305 major world river basins and will indicate the predicted river flow anomaly and its probability of occurrence across the global river network. Clicking on a basin will call up hydrographs showing the ensemble river flow forecast out to four months, including the relevant climatological thresholds for the time of year. If the forecast exceeds/falls below them, the maximum/minimum weekly discharge from the entire climatology and the month and year in which this occurred are also shown.

During pre-operational testing in December 2016, GloFAS-Seasonal was able to pick up a signal of the devastating flooding that occurred in Peru from late January to March 2017. While the uncertainty was large, almost the entire ensemble indicated river flow exceeding the 90th percentile. Such forecasts, provided weeks to months ahead, could allow movement of resources and preparation of aid in advance of flood or drought events.



EFAS seasonal outlook initialised on 1 April 2017. The map (left) indicates the probability of abnormally high (blue) or low (red) flows during the next eight weeks; the darker the colour, the higher the probability. The hydrograph (right) shows the river flow forecast for the Angerman River basin (Sweden), and how the forecast compares to the river flow climatology. The percentage of ensemble members below/above the 10th/90th percentile of the entire pseudo-observed river flow climatology is shown (red/blue numbers) when >50%. The current pseudo-observed river flow ('water balance') is added to the hydrograph once available.



Prototype GloFAS-Seasonal forecast from December 2016. The map indicates the probability of abnormally high (blue) or low (orange) flows during the next 4 months; the darker the colour, the higher the probability. The hydrograph (inset) shows the river flow forecast out to 4 months for Peru, and how this compares to typical and extreme conditions, based on the river flow climatology (produced by running ERA-Interim-Land through GloFAS). The forecast shown here is a prototype of the final visualisation of the GloFAS-Seasonal product, which will become publicly available via www.globalfloods.eu in autumn 2017. If you have any feedback, suggestions or comments, please email rebecca.emerton@ecmwf.int or comment on the relevant page in the GloFAS Confluence space.

Flood forecast decision-making games

LOUISE ARNAL, FREDRIK WETTERHALL, FLORIAN PAPPENBERGER

The HEPEX (Hydrological Ensemble Prediction Experiment) community is a network of scientists and practitioners who aim to promote and develop ensemble hydrological forecasting. ECMWF has been a driving force behind HEPEX from the start and is involved in a range of HEPEX activities, including the development of serious games. These are a great teaching tool as they can convey what is involved in complex real-world decisions in an interactive setup and with an easy-to-understand message. They are designed to promote the use of probabilistic forecasts in decision-making for applications such as reservoir management and flood protection.

HEPEX games have been developed by scientists from ECMWF, the University of Reading, the French Institut national de recherche en sciences et technologies pour l'environnement et l'agriculture (Irstea), the Red Cross/Red Crescent Climate Centre and the IHE Delft Institute for Water Education, among others. They have been played at European Geosciences Union General Assemblies as well as workshops and training courses at ECMWF. Below we present two games developed in 2015 and 2017. For a full list of games, visit: <https://hepex.irstea.fr/resources/>.

How much are you willing to pay for a forecast?

The 2015 game 'How much are you willing to pay for a forecast?' was designed to look at the perceived value of probabilistic forecasts by decision-makers for flood protection.

In this game, the participants are given probabilistic forecasts of the river level, based on which they have to decide whether to buy flood protection for an imaginary town. The forecasts are of varied quality (positively or negatively biased, or unbiased) and each participant is randomly given a certain forecast quality type, without their knowledge. The participants' willingness to pay for probabilistic



Playing the game. Teams playing 'Pathways to running a flood forecasting centre: an adventure game' at the IMPREX 2017 General Assembly at ECMWF.

forecasts is also evaluated during the game through an auction, as forecasts in a second part of the game are no longer given out but sold, and in a limited number. To mention a few key results from the 129 collected game sheets (more results can be found in an article by *Arnal et al.* in *Hydrol. Earth Syst. Sci.*, 2016, doi:10.5194/hess-20-3109-2016):

- The perceived risk (driven by the river flood frequency, the initial river level and the proximity of the predicted river level to the flood threshold) as well as the perceived forecast bias influenced the participants' use of the forecasts (i.e. the percentile of the forecast on which decisions were based).
- The participants' willingness to pay for probabilistic forecasts was strongly linked to their perception of the quality of the forecasts. Interestingly, the participants' perception of their own performance as decision-makers was also highly correlated with their perception of the forecasts' quality (perceptions evaluated with a questionnaire at the end of the game).
- Overall, this game showed that the use and perceived value of probabilistic forecasts for decision-making in a risk-based context is not straightforward. More work is needed to provide

comprehensive guidance on the use of probabilistic information for decision-making, by communicating the quality as well as the relevance and long-term economic benefit of probabilistic forecasts for improved decisions.

Pathways to running a flood forecasting centre: an adventure game

The 2017 game 'Pathways to running a flood forecasting centre: an adventure game' aims to explore the decision-making process involved in running a flood forecasting centre.

In this game, the participant is the head of a flood forecasting centre and has to protect a town against floods with the help of two teams: forecasters and the flood incident response team. The participant can interact with the teams (such as to get advice and information or ask them to perform certain actions, e.g. installing flood defences or improving the forecast) and access probabilistic forecasts of the river level. The participant is ultimately responsible for all actions and their consequences, which will impact her/his budget and reputation.

The results of this game will be reported in a HEPEX blog post as well as in a scientific article. This game is available to play online at: <https://goo.gl/bfZISB>.

ECMWF meets its users: UEF 2017

**ANNA GHELLI,
FLORIAN PAPPENBERGER**

More than 100 forecasters and scientists attended this year's Using ECMWF's Forecasts (UEF) meeting, which took place at the Centre from 12 to 16 June 2017. They heard about ECMWF's plans for future products, services and research and were able to network and share experiences with participants from other countries. Activities ranged from oral presentations, posters and demonstrations to hands-on sessions. The demonstrations provided an opportunity to show and try out software or services developed at institutions based in ECMWF's Member and Co-operating States.

UEF is one of the channels for ECMWF data users to provide feedback on products and services and to request new products. For the last three years this has been done successfully through the 'User Voice Corner'. At the end of the meeting, user voices are collated and they subsequently feed into ECMWF's future plans.

Storms

The theme of this year's UEF was 'storms'. Severe storms, whether they happen in winter or summer, have considerable impact on people's lives and may lead to significant disruption to services and commercial activities. They can come with not just strong winds and heavy rain but also hail, lightning, blizzards, floods and storm surges. These can lead to damage and destruction of infrastructure, injury and death. Predicting the onset, intensity and track of severe storms with enough lead time is therefore essential for

readiness and damage limitation. Moreover, some applications may require information on weather regime changes in the extended-range forecast, such as the prospect of a stormy period two weeks ahead, or seasonal outlooks.

Numerical weather prediction (NWP) models support meteorological services with forecasts of when a storm will form, where it will strike and how severe it will be, and with an indication of the degree of confidence we can have in the forecast. ECMWF has been at the forefront of NWP development for many years and our Strategy includes the provision of high-quality severe weather forecast products.

The meeting focused on three thematic areas:

- Processing of model outputs to support the forecasting of severe storms and associated weather phenomena.
- Diagnostics involving tools or studies that highlight strengths and weaknesses of ECMWF's Integrated Forecasting System (IFS) in predicting storms.
- Impact of storms on sectoral applications.

Meeting highlights

"Providing model output which is useful and supports the work of our Member and Co-operating States is at the heart of ECMWF's Strategy," said Director of Forecasts Florian Pappenberger in the opening lecture of the UEF. He also provided a timeline of IFS upgrades with particular emphasis on IFS Cycle 43r3 implemented on 11 July 2017. A number of products aimed at supporting forecasting activities were also shown. They included the probability of

Workshop: Storm naming – does it work?

Gerald Flemming (Met Éireann) and Will Lang (Met Office) ran this workshop to share the experience of a collaborative project between the two meteorological services initiated in 2015. The project started as a pilot initiative to investigate the effect of 'naming' large-scale mid-latitude windstorms on the reach and influence of severe weather advice for the UK and Ireland. Gerald and Will started the workshop by asking the participants how they would describe themselves if they could not say their names. It was a rather difficult exercise, which highlighted the importance of a name as an identifier for a person. Similarly, a named storm will allow the audience to focus more on its potential impact on their lives. The workshop also aimed to collect feedback on how the scheme could help end users to benefit from improved NWP capabilities and how it could enhance the authoritative voice of European national meteorological services.

precipitation type, point rainfall, distributions for the monthly forecast, moisture flux and regime transitions.

Ensemble forecasting was presented in many talks: Helen Titley from the UK Met Office gave an invited talk on processing ensemble information. She showed a variety of tailored applications available to Met Office operational meteorologists



Workshop participants. More than 100 forecasters and scientists attended this year's UEF meeting.



Weather wall demonstration.

The meeting included activities ranging from oral presentations and posters to demonstrations and hands-on sessions.

based on both ECMWF and Met Office ensemble forecast data to help forecast severe extratropical cyclones.

“Predicting high-impact weather events is a crucial task for forecasting centres,” said ECMWF scientist Linus Magnusson. He presented examples of evaluation and diagnostics that can be used to understand the predictability of severe events and stressed the importance of identifying key features in the development of severe weather that can be verified to improve the IFS. During his contribution, ECMWF’s review of headlines scores to assess forecast performance was mentioned. The review ties in with ECMWF’s Strategy to 2025, which calls for ensemble forecasts at 5 km resolution. Lara Gunn from MetDesk showed how ECMWF data are used to provide tailored forecasts for the transport

and energy sectors. She reminded the audience that heavy rain in the Alps has an impact on Alpine reservoirs and the upper Danube, which in turn affects energy production across France and Eastern Europe. Being able to predict these kinds of event with high accuracy is thus of great importance for fragile European markets.

A presentation from the European Severe Storms Laboratory (ESSL), which organises the annual ESSL Testbed event, showed how the laboratory is used to train forecasters in predicting severe convective storms using state-of-the-art forecasting tools. ESSL can also facilitate the evaluation of experimental and/or new forecast products based on numerical weather prediction models as well as radar and satellites. ECMWF is a member of ESSL.

Paul Knightley (MeteoGroup) presented

some fascinating videos and photos of storms mainly from his own storm chasing trips. *“Storm chasing is really exciting,”* said Paul, *“but you have to be really patient. You have to stay put in a place and wait for the storm to form.”* While seeing a storm form and following it is really rewarding, it can also be a terrifying experience as the course of the storm may deviate from the expected path and threaten properties and lives.

EUMETSAT

This year EUMETSAT contributed with a plenary talk and a workshop on satellite data and products as storm monitoring tools and as input into data assimilation schemes. Satellite and conventional data are critical to the development and improvement of NWP. ECMWF and EUMETSAT have worked closely together to demonstrate the value of new satellite observations and to ensure maximum benefit for Member and Co-operating States from investments in the satellite programme.

EUMETSAT has provided its user community with more than three decades’ worth of satellite data. Its current programmes include the procurement and future operation of Meteosat Third Generation (MTG) satellites and EUMETSAT Polar System Second Generation (EPS-SG) satellites. The Infrared Sounder on MTG will provide information with the potential to improve forecasts of severe weather events. In preliminary studies the sounder has been shown to be able to detect the initiation of atmospheric rivers, which are long, narrow and transient corridors of strong horizontal water vapour transport. Such rivers are usually associated with a low-level jet stream ahead of a cold front or an extratropical cyclone. They produce heavy precipitation where they are forced upwards.

Visualising ensemble forecasts

During the UEF 2016 we launched ‘The Challenge’: ECMWF data users could submit proposals to improve the way probabilistic information and in particular the popular ENS Meteogram is displayed. The Challenge was won by Dave MacLeod, Hannah Christensen, Stephen Juriche and Aneesh Subramanian with an entry based on the philosophy of progressive disclosure of information. We would like to thank all those who submitted a proposal and congratulate the winners.

Workshop: Hazard impact modelling for storms

“Participants were encouraged to think about opportunities for impact prediction and risk-based warnings and services,” Ken Mylne from the UK Met Office explains. During the workshop many different weather-related impacts were discussed. Some of the key ideas were that impact predictions are powerful tools in supporting effective communication and helping decision-makers to understand the situation, but that they may still require expert interpretation.

Historical impacts of weather of any type can be related to particular weather regimes, giving probabilities of impact depending on regime

occurrence. Global ensembles are ideal for predicting the probabilities of regime occurrence, enabling the prediction of heightened risks of impacts without the need for high-resolution ensembles.

Storms have an impact on transport and power distribution networks. Vulnerabilities in these sectors vary greatly. It is therefore important to use ensemble forecasting systems at higher resolution. Enhanced diagnostics of precipitation type like those developed at ECMWF will help with downscaling in conjunction with high-resolution mapping of transport networks and power distribution networks.

Record numbers attend ECMWF's NWP courses

SARAH KEELEY

This year a record number of more than 150 participants attended ECMWF's advanced numerical weather prediction (NWP) courses. These unique courses are designed to meet some of the training needs of ECMWF's Member and Co-operating States. They focus on the underlying theory of numerical weather prediction but relate it to an operational setting, with an emphasis on processes relevant for forecasting from the medium to seasonal time range. Much of the course material is theoretical but we include practical and discussion sessions to build on what is presented in lectures and consolidate understanding. The face-to-face training courses provide a networking hub for researchers and forecasters to exchange ideas with each other and ECMWF staff. One of the key pieces of feedback we receive each year from attendees is how much they appreciate the time research staff give to them informally during the course. Discussions during coffee breaks and evening social events mean that the learning and networking goes beyond the time spent in the classroom. Our courses also benefit from collaboration. For example, we have been able to expand the training devoted to the research area of satellite data assimilation through the co-funding provided by EUMETSAT through their NWP-SAF programme. In addition, the UK's National



ECMWF's classroom. The NWP training courses combine lectures with practical and discussion sessions.

Centre for Earth Observation based at the University of Reading runs an introductory two-day training course on data assimilation ahead of our more advanced course.

We also share the training materials for those unable to attend the courses in a face-to-face setting. Some participants attend the course to help them develop their own training programmes. Lecture handouts are publicly available after the course in the Learning section of the ECMWF website (www.ecmwf.int/en/learning/education-material). Next year some of the courses will benefit from

the eLearning modules being produced and will be delivered in a blended format: some pre-course study will be undertaken using the new online modules rather than just pre-course reading.

The deadline for training course applications is 28 September 2017. This is earlier than in previous years so that confirmation notices can go out earlier, which should help to keep down travel and accommodation costs for participants. Descriptions of the courses and how to apply can be found at www.ecmwf.int/en/learning/training.

NWP courses for 2018

Data assimilation	12–16 March 2018
EUMETSAT/ECMWF NWP-SAF Satellite data assimilation	19–23 March 2018
Advanced numerical methods for Earth system modelling	16–20 April 2018
Parametrization of subgrid physical processes	23–27 April 2018
Predictability and ensemble forecast systems	30 April – 4 May 2018

Participant feedback from this year's courses

"Despite being already experienced on these topics, I found the course very instructive. Other than being exceptional scientists, lecturers demonstrated that they are effective teachers, and classes were overall very useful for my career. I have no other suggestion, except for saying: Keep going this way!"

"A very full but interesting course. Practical sessions and/or audience participation helped to drive home many of the messages. Very friendly and good lecturers. Thanks for a very informative and good week!"

ECMWF air quality data competition has a winner

CLAUDIA VITOLO, MIHA RAZINGER, PIOTR KUCHTA

The winner of an ECMWF-organised Kaggle in Class competition on ‘Predicting the impact of air quality on mortality rates’, Matthias Gehrig from Germany, was announced on 5 May 2017. Matthias did a fantastic job tackling this challenge: after 60 submissions he scored a root-mean-square error of 0.29023 on the private leaderboard just 12 minutes before the competition’s deadline. After the competition he revealed that he used a simple Excel spreadsheet and public leaderboard feedback to model the mortality trend, which he then used as input to xgboost, along with other features derived from the input data provided. The xgboost library implements eXtreme Gradient Boosting, a scalable tree boosting algorithm widely used by data scientists and winners of other Kaggle machine learning competitions.

Wide range of strategies

Poor air quality is a significant public health issue. According to a COMEAP (UK Committee on the Medical Effects of Air Pollutants) report, the burden of particulate air pollution in the UK in 2008 was estimated to be equivalent to “nearly 29,000 deaths at typical ages and an associated loss of population life of 340,000 life years”. The goal of the competition was to predict mortality rates due to cardiovascular and respiratory diseases and cancer for each English region using daily means of temperature and ozone (O₃), nitrogen dioxide (NO₂), PM₁₀ (particulate matter with a diameter of less than or equal to 10 micrometres)

and PM_{2.5} (2.5 micrometres or less) surface concentration. The competition attracted 51 data enthusiasts, from beginners to Kaggle Grandmasters, from several countries including China, India, Mexico, the United Kingdom, France, Germany and Poland. Some of them actively participated in the forum discussions highlighting the challenges the data posed. The modelling strategies adopted varied widely, even the choice of the most important predictors seemed to be very different across submissions. Some pointed out that environmental factors (such as pollution concentrations) were less influential than temporal trends. Many considered that handling missing values was the most challenging part of the competition. The competition’s organisers provided background information on the data and sample code. This helped first-time Kagglers (about 25% of the participants), who said that ‘it was easy to get started’. The example code was provided in two programming languages: Python and R. These were the two main tools used by the participants. Additional information and alternative modelling strategies were discussed in the forum, which was considered useful by the majority of participants.

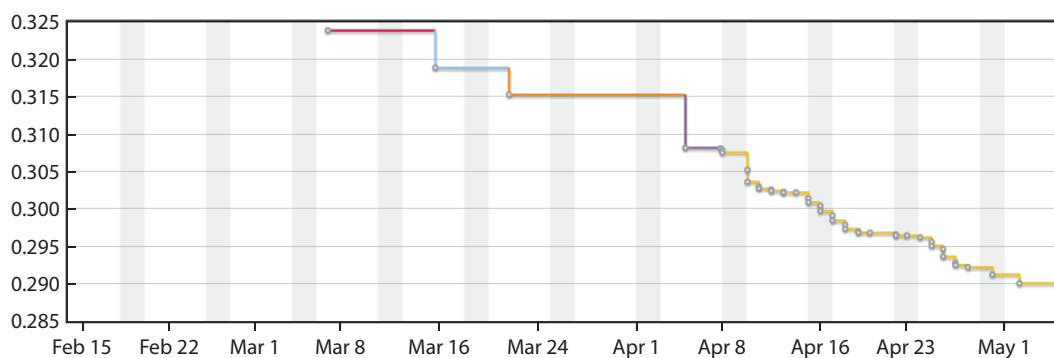
Promoting data use

The Kaggle competition is one of several outreach activities to promote data from ECMWF and the EU’s Copernicus Earth observation programme. It was launched on the last day of the Open Data Week held at ECMWF earlier this year. Some of the public datasets provided by the ECMWF-run Copernicus Atmosphere Monitoring Service (CAMS regional

reanalysis) were used to assemble predictors (temperature and pollutant concentrations) for training and testing competition data. The outcome variable was obtained from mortality and population counts for the English regions provided by the UK’s Office for National Statistics.

The competition was designed to reach out to a new audience: the exploding number of data scientists and data enthusiasts across the world. Introducing some of the ECMWF and Copernicus open datasets to a wider audience could help to unleash their potential and encourage their use in fields not directly related to weather and climate. At the same time, showcasing machine learning approaches, which are domain agnostic, provides a novel perspective and generated interest among ECMWF staff and the weather and climate community.

The design of a data science competition is, however, not straightforward. Kaggle provides an infrastructure for competitions at different levels of complexity. In the lower range there are Kaggle in Class competitions, in which both training and testing data can be in the public domain and there is no monetary prize. We opted for this category for two reasons: we only used open datasets and wanted to ensure the competition was beginner friendly. In the future, we plan to also run advanced competitions with monetary prizes. These generally draw more attention, especially by expert kagglers, but they can only be set up using private datasets for the outcome variable. Suggestions are welcome!



Competition leaderboard. This was a particularly tough competition. The top score shown on the competition leaderboard improved only slightly in the final three weeks before it reached the final value of 0.29023.

A fresh look at tropical cyclone intensity estimates

LINUS MAGNUSSON, MOHAMED DAHOU (both ECMWF), **CHRISTOPHER S. VELDEN, TIMOTHY L. OLANDER** (both University of Wisconsin)

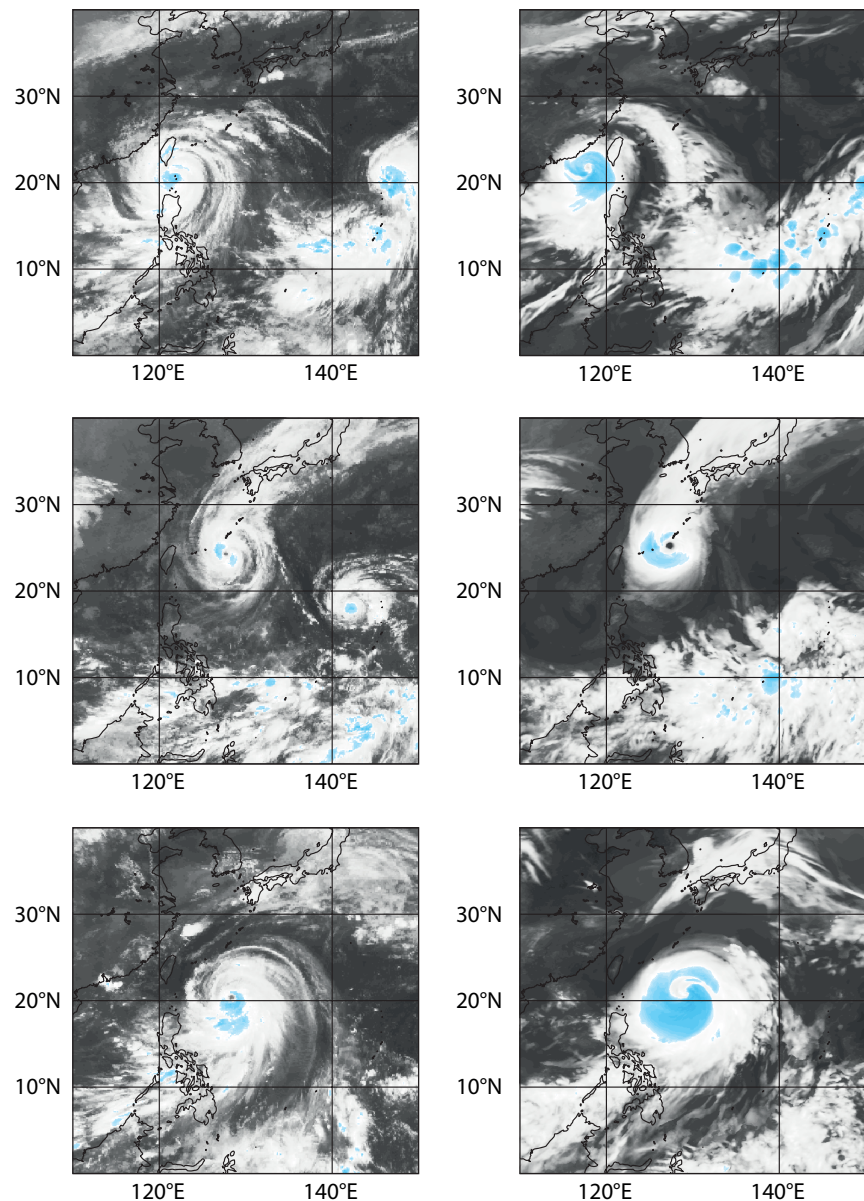
In the absence of suitable observations, the verification of tropical cyclone (TC) intensity predictions traditionally relies on estimates of wind speeds and mean sea level pressure (MSLP) at the centre of TCs. These estimates are usually derived from satellite observations of cloud structure using the Advanced Dvorak Technique (ADT). The ADT method has been assessed in dedicated studies by comparing the estimates with in-situ measurements by aircraft reconnaissance. A new way of assessing it uses simulated satellite images produced at ECMWF.

The ADT method

The ADT method, mainly developed at the University of Wisconsin, uses observations from the longwave infrared window channel to derive an intensity classification referred to as the 'T number'. The T number is calculated by exploiting empirical relationships between the image scene characteristics and TC intensity. However, uncertainties in the estimation arise from the empirical relationship between cloud patterns and the T number and from the translation of the T number into minimum MSLP and maximum wind speed. Traditionally ADT performance has been assessed by comparing ADT results with in-situ observations obtained by aircraft reconnaissance. Since such assessments are limited by the availability of in-situ observations, we here present an alternative based on simulated satellite images from ECMWF forecasts.

Assessing ADT estimates

We assume that there is a good level of consistency between simulated satellite images and the predicted intensity (expressed in terms of MSLP or maximum wind) since both are generated by the same model. Finding good consistency between the ADT results from simulated images on the one hand and the model surface fields on the other would thus provide additional confidence in the behaviour of the ADT algorithm as well as in the simulated satellite images.



Real and simulated satellite images. Observed images from Himawari-7 with 4 km resolution (left) and simulated satellite images from 4-day forecasts with 9 km resolution (right) for TC Usagi valid at 00 UTC 23 September 2013 (top), TC Fitow valid at 00 UTC 5 October 2013 (middle) and TC Neoguri valid at 00 UTC 7 July 2014 (bottom).

Since 2016 ECMWF has been producing simulated satellite images with global coverage. These are generated using the operational high-resolution forecast model and the radiative transfer model used in the operational data assimilation (e.g. RTTOV 11). The output from the model is used as input to RTTOV to derive and simulate the brightness temperatures that geostationary satellites would observe given the relevant model profiles and surface parameters.

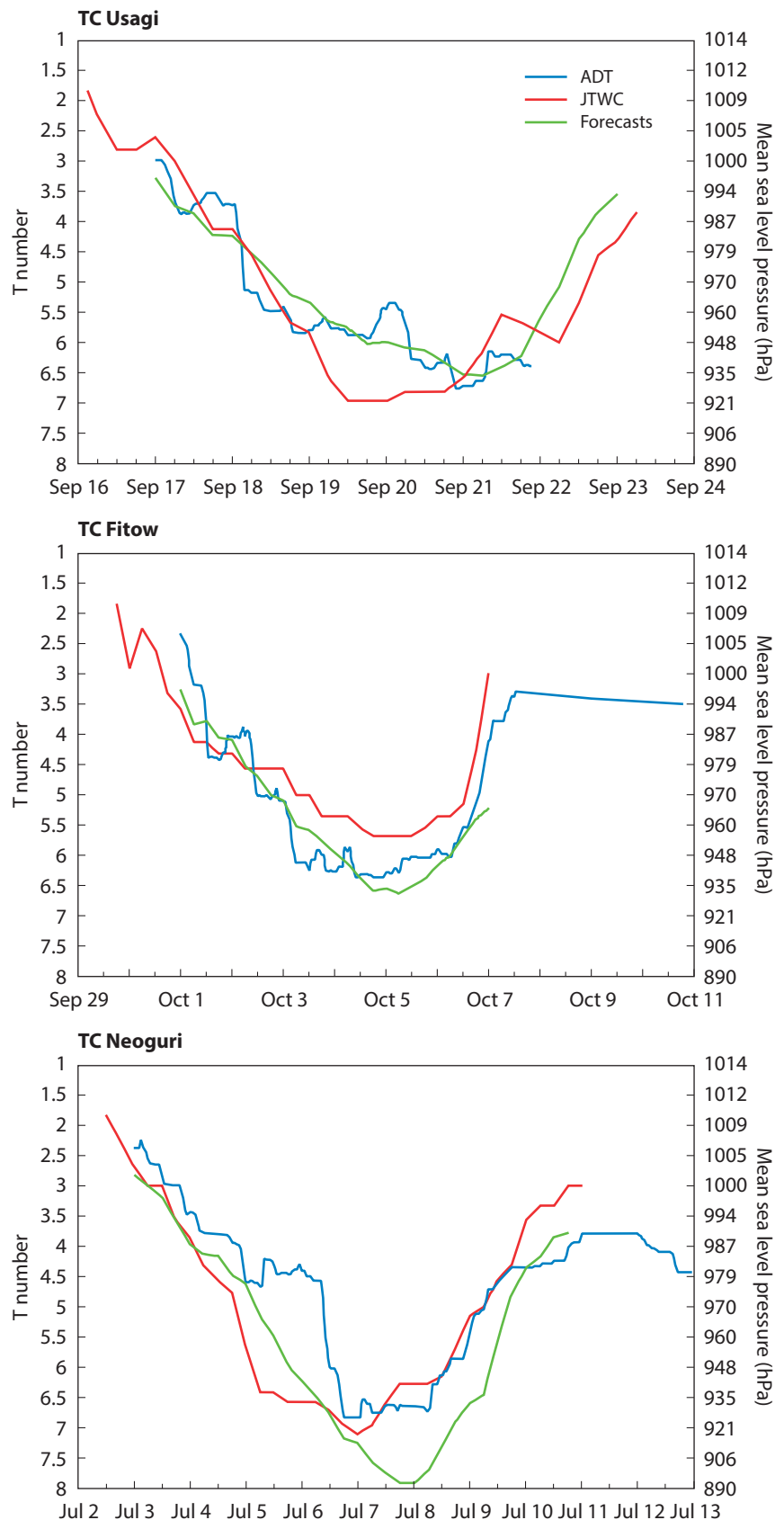
Such images are routinely produced from the model in both the infrared atmospheric window and water vapour regions at three-hourly intervals. In this pilot study, images of TC Usagi (2013), Fitow (2013) and Neoguri (2014) have been used as input for the ADT. The resulting intensity estimates in terms of minimum MSLP can be compared with the minimum MSLP predicted by the model. The results, shown in the line charts (blue and green lines), agree well

with each other for most of the time steps for these three cases. However, they differ for the most intensive phase of TC Neoguri. This is expected as the modelled cyclone is very deep and only few cyclones this deep have occurred in reality, making the statistical relations used in the ADT method uncertain. Particularly large differences are found for TC Neoguri during the intensification phase, where the estimated intensity from the simulated images using ADT is much less than the intensity predicted by the model. One explanation is that the cirrus canopy can obscure TC structure underneath as the vortex organization improves, thereby creating a false plateau in the intensity estimates derived from the IR scenes. In such conditions, the availability of polar-orbiting satellite microwave (MW) images can be used to aid in the detection of the developing eye. Unfortunately, model-simulated MW imagery was not available for use in the ADT method in this study.

The preliminary results of the study show that in most cases the ADT algorithm provides relatively good estimates of modelled intensities in terms of MSLP using the model-simulated satellite data as input. In terms of maximum wind, in nearly all cases the ADT intensities are stronger compared to the model forecast wind estimates (10-minute average winds – not shown). This is in line with previous findings, which show that ECMWF forecasts significantly underestimate time-averaged surface winds, especially for intense cyclones.

The pilot study results also show a good correlation between intensity estimates derived by the Hawaii-based Joint Typhoon Warning Center (JTWC), who use the Dvorak technique, and simulated ADT results. This is the case even during episodes of rapid intensification even though the time phasing may differ.

A potential future direction is to systematically compare model-simulated satellite images with real satellite images to verify tropical cyclone intensities. This would provide a more direct comparison between modelled and observed quantities than just comparing minimum pressure or maximum wind plots against estimates from JTWC and other tropical cyclone agencies. However, this would require model-simulated satellite images with hourly resolution and the inclusion of simulated MW imagery.



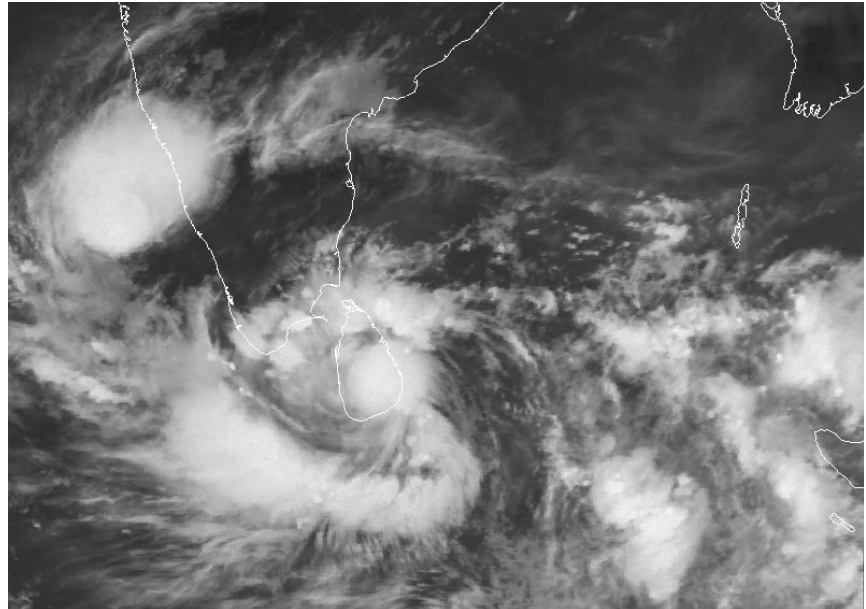
Comparison of model predictions with intensity estimates based on simulated images. The charts show ADT intensity estimates based on simulated satellite images, predicted intensity in ECMWF forecasts of MSLP and JTWC intensity estimates for TC Usagi (top), TC Fitow (middle) and TC Neoguri (bottom).

ECMWF helps to upgrade Sri Lankan forecasting capability

**UMBERTO MODIGLIANI,
FABIO VENUTI**

After long negotiations with the help of the World Meteorological Organization (WMO), ECMWF has signed a new full NMHS (national meteorological and hydrological service) non-commercial licence with Sri Lanka. The contract is for two years starting on 1 July. Sri Lanka has access to both data and web products including ecCharts. The licence is part of an effort to upgrade Sri Lankan operational forecasting capabilities with the support of donor agencies. The World Bank is supporting this work and Met Norway is involved with technical assistance. The ECMWF products will help Sri Lanka to respond better to severe weather events, such as Tropical Cyclone Roanu on 16 May 2016, which caused flooding and landslides resulting in loss of life and significant damage.

Eleven countries now have a full NMHS non-commercial licence: China, Colombia, Hong Kong, Indonesia, Macao, Mexico, Republic of Korea, Saudi Arabia, Sri Lanka,



Tropical Cyclone Roanu. This Meteosat-7 infrared satellite image from 15 May 2016 03 UTC shows a large storm cloud over Sri Lanka associated with the developing Tropical Cyclone Roanu. (Copyright 2017: EUMETSAT)

Singapore, and Viet Nam.

The price for a full NMHS non-commercial licence is 42,000 euros per year. For more information on the

available licences, see the ECMWF licences web page: <https://www.ecmwf.int/en/forecasts/accessing-forecasts/licences-available>.

End of the road for GRIB-API

**UMBERTO MODIGLIANI,
SHAHRAM NAJM,
STEPHAN SIEMEN,
DANIEL VARELA SANTOALLA**



ecCodes has become the default decoder/encoder for the binary data format GRIB at ECMWF. All the main operational systems, the Integrated Forecasting System and software packages at ECMWF, have now been migrated to ecCodes. We are confident that ecCodes can replace GRIB-API for all GRIB decoding/encoding activities

and strongly suggest that users test and migrate their applications to ecCodes at the earliest opportunity.

ecCodes is an evolution of the GRIB-API software package with extended functionality and the ability to also handle data in BUFR format. The existing API function names, header files and tools starting with the string "grib_" will continue to exist and this will facilitate the migration. More details on ecCodes can be found in ECMWF Newsletter No. 146, winter 2015/16.

Please note that no new features or functionality will be implemented in GRIB-API, and in the coming months only major or critical bug fixes and support for new parameters will be provided. Any existing and future feature request for GRIB data handling will only be addressed in ecCodes. ECMWF plans

to cease all development work on GRIB-API at the end of 2018. After this time no further changes will be made to GRIB-API. ECMWF will install just ecCodes on new ECMWF platforms, such as the next supercomputer.

Please contact Software Support (software.support@ecmwf.int) if you have any queries.

Useful web links

ecCodes: <https://software.ecmwf.int/wiki/display/ECC>

GRIB-API: <https://software.ecmwf.int/wiki/display/GRIB>

Differences between GRIB-API and ecCodes: <https://software.ecmwf.int/wiki/display/ECC/GRIB-API+migration>

New IFS version control and issue tracking tools

MICHAEL SLEIGH, ROBERTO BUIZZA, PAUL BURTON, RICHARD FORBES, DANIEL VARELA SANTOALLA, TOMAS WILHELMSSON

As part of continuous efforts to improve our software infrastructure, and therefore research productivity, we have migrated the Integrated Forecasting System (IFS) code from the Perforce version control system (VCS) to Git. We have also introduced the JIRA tool for issue tracking and software management.

Git

The migration to Git was started during the development of IFS Cycle 43r3, which was implemented on 11 July 2017 (see separate article in this Newsletter). In a phased approach, researchers developed their individual contributions under Perforce, but then the branches were imported into Git, which was used to produce the final build. IFS-specific extensions to Git were developed and tested during this period. The next operational cycle, 45r1, will be the first to be developed end-to-end in Git.

Git has several advantages for ECMWF and Member State developers of the IFS. As it is a distributed rather than centralised VCS, each developer holds their own copy of the full repository, complete with its entire history. Consequently most version control operations are local and do not involve communication with a central server. Hence:

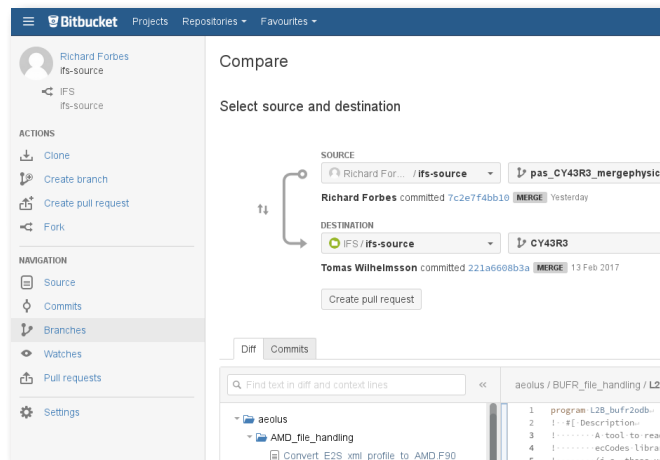
- Performance will not degrade with the size of the repository or number of users

Useful links

Both the Bitbucket web interface to the IFS code and the IFS JIRA site are available to users outside ECMWF who have been granted the 'ifs' access policy, at: <https://software.ecmwf.int/stash/projects/IFS> and <https://software.ecmwf.int/issues/projects/IFS>, respectively.

For more information on Git, visit: <https://git-scm.com>

For more information on JIRA, visit: <https://www.atlassian.com/software/jira>



Bitbucket suite. ECMWF uses Bitbucket to host all its software, including now the IFS.

- Committing changes, creating branches and merging are much faster, which will encourage better software development habits
- Git can be used without network access – a connection to the server is needed only to share work with others, which happens less often
- Developers can work locally on multiple machines, e.g. when hot-desking or travelling
- There is more control over sharing, leading to a cleaner organisation of branches, rather than a single repository with tens of thousands of branches exposed to every user.

Moreover, Git is free software, thus opening the possibility of cost savings. It is also widely known, thus facilitating sharing code with other organisations and accepting external contributions.

JIRA

Starting with Cycle 43r3, we have also taken the opportunity to introduce JIRA, a web-based issue tracking and software project management application. JIRA is part of the same suite as Bitbucket, which ECMWF already uses to host all its software (including now the IFS, as a result of the Git migration), and Confluence, which ECMWF uses as a wiki and to host its intranet.

This now provides a central repository of information for IFS development. It documents modifications, from bug fixes to major scientific improvements, in a systematic way, providing a widely available, transparent, searchable database. Each code change is logged

with information about the change, its interactions with other developments, the testing and evaluation that has been performed, and other details such as dependencies on other software components. This leads to much more transparency and clarity about what work is being done, by whom, and what state it is in. ECMWF already hosts its User Request Management System in JIRA, so now an IFS code change for a new output parameter, for example, can be linked within JIRA to the Member State request, giving a full line of sight. It can also be linked to Data Governance requests, to ensure these inter-dependencies are managed.

This new system will facilitate project management and delivery of cycles; improve communication within and between ECMWF departments, Member and Co-operating States, and external collaborators; and centralise and streamline IFS-related documentation.

Next steps

The next stage in the modernisation of the IFS infrastructure is to replace the existing build system with ecBuild, which is ECMWF's generic build tool based on CMake. This will greatly simplify and speed up the IFS build process. It will also enable a full IFS build to be performed on a workstation or continuous integration server. Subsequently, therefore, the combination of Git and ecBuild opens the way to automated technical testing to help find and fix bugs more quickly.

IFS Cycle 43r3 brings model and assimilation updates

ROBERTO BUIZZA, PETER BECHTOLD,
MASSIMO BONAVITA, NIELS BORMANN,
ALESSIO BOZZO, THOMAS HAIDEN, ROBIN HOGAN,
ELIAS HOLM, GABOR RADNOTI, DAVID RICHARDSON,
MICHAEL SLEIGH

On 11 July 2017, ECMWF implemented a substantial upgrade of its Integrated Forecasting System. IFS Cycle 43r3 includes changes in the model; in the way observations are used; in software infrastructure; and in the assimilation procedure used to generate the initial conditions for forecasts. The upgrade has had a broadly positive impact on forecast skill in medium-range and monthly forecasts. It follows the implementation of IFS Cycle 43r1 in November 2016, which for the first time included an interactive sea-ice model in the medium-range/monthly ensemble (Buizza *et al.*, 2017). Cycle 43r3 brings major changes in many areas, including:

- **In assimilation:** improved humidity background error variances directly from the Ensemble of Data Assimilations (EDA), like for all other variables; revised wavelet filtering of background error variances and revised quality control of dropsonde wind observations in the data assimilation to improve tropical cyclone structures
- **In the use of observations:** increased use of microwave humidity sounding data by adding new sensors; harmonised data usage over land and sea ice for microwave observations; improved screening of infrared observations for anomalously high atmospheric concentrations of hydrogen cyanide from wildfires; improved quality control for radio occultation observations and radiosonde data
- **In the model:** a new, more efficient radiation scheme with reduced noise and a more accurate longwave radiation transfer calculation; a new aerosol climatology including dependence on relative humidity, derived from data provided by the Copernicus Atmosphere Monitoring Service (CAMS); increased super-cooled liquid water at colder temperatures from the convection scheme; visibility calculation changed to use the new aerosol climatology
- **In software infrastructure:** new version control and software management tools; changes to enable single-precision experiments for all applications.

Expected impacts

A comparison of parallel runs of the previous operational cycle (43r1) and the new cycle (43r3) indicates in general a positive impact. As a result of the changes in data assimilation and in the way dropsonde observations are handled, analyses are expected to improve, especially in

the case of tropical cyclones.

Results for both the high-resolution forecast (HRES) and the medium-range/monthly ensemble (ENS) indicate a positive impact, with many of the scores over the northern and southern hemispheres (NH, SH) and Europe indicating statistically significant improvements. Improvements are larger in summer than in winter. Changes to the deep convection scheme have improved the temperature gradient between the extratropics and the tropics. Significant improvements are found for temperature and vector wind throughout the extratropical troposphere. In the tropics, there is some deterioration in temperature and humidity at certain vertical levels associated with the changes to the deep convection scheme.

Considering the HRES, statistically significant improvements at the 95% level have been detected up to about forecast day 5 when forecasts are verified against the analysis. When forecasts are verified against observations, the positive impact of 43r3 is also evident. Surface parameters show partially statistically significant improvements both in the tropics and extratropics (2 m humidity, 10 m wind speed, total cloud cover, precipitation), except for 2 m temperature, which shows neutral results. Over the ocean, statistically significant improvements are seen for verification against the analysis for 10 m wind speed, significant wave height and mean wave period.

Results for ENS indicate mainly a positive impact similar to HRES both for upper-air and surface variables for the NH, SH, and Europe when verified against the analysis. In the tropics, there is some deterioration in upper tropospheric wind speed and lower tropospheric temperature associated with reduced spread. There is also some slight deterioration in tropical 2 m temperature and precipitation scores.

Changes in the tropical cyclone analysis are notable, with the cyclone structure defined in a better way. At forecast day 1 there is a marginally significant improvement in position error; the improvement is undetectable thereafter. Tropical cyclone intensity (as measured by central pressure) is slightly reduced from day 2 onwards: for lead times beyond four days this has a beneficial effect since it reduces the existing bias in tropical cyclone central pressure in such forecasts.

Figure 1 shows the HRES scorecard of Cycle 43r3 versus Cycle 43r1, based on experiments covering 740 forecasts from June 2016 to June 2017. It also shows the corresponding ENS scorecard for medium-range/monthly forecasts up to forecast day 15, based on 170 cases.

Data assimilation

In Cycle 43r3 two significant upgrades in the 4-dimensional variational assimilation configuration (4DVAR) have been implemented. The first involves using background

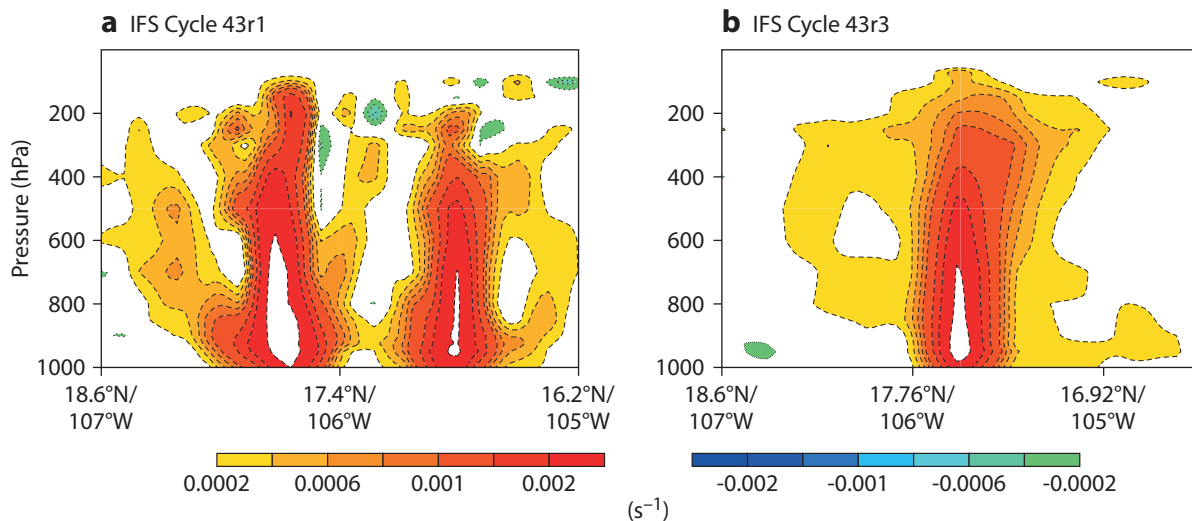


Figure 2 Tropical cyclone high-resolution analysis of relative vorticity (cross section) for 12 UTC on 23 October 2015 produced using (a) the previous IFS cycle, 43r1, and (b) IFS Cycle 43r3. In IFS Cycle 43r3, there is a more cautious use of dropsonde wind observations by means of adaptive observation error and smoother filtering of the EDA background error variances.

humidity error estimates sampled from the Ensemble of Data Assimilations (EDA) in the 4DVAR analyses (both in the high-resolution version and in the EDA itself) instead of the previously used statistical model. This change makes the treatment of humidity background errors consistent with the rest of the control vector and makes the error estimates more flow dependent. The humidity error change has led to improvements in the forecast fit to humidity-sensitive observations and to reductions in wind vector forecast errors. In addition, the updated climatological background error statistics (B matrix) improve the forecast fit to stratospheric satellite data.

The second upgrade involves the way observations

are assimilated and the weight given to dropsonde observations near the centre of tropical cyclones. Previously the analysis of tropical cyclones occasionally showed unrealistic features (e.g. double centres, elongated cores). These problems were tracked to unrealistic observation error values assigned to dropsonde observations, and to the increase in the resolution of the EDA background errors adopted in Cycle 43r1. The upgrade has improved the tropical cyclone initialisation by introducing an adaptive observation error model for dropsonde measurements and a smoother filtering of the background error. The latter was achieved by spectrally truncating the errors to TL159 instead of TL399 and applying a new wavelet instead of spectral signal-to-noise

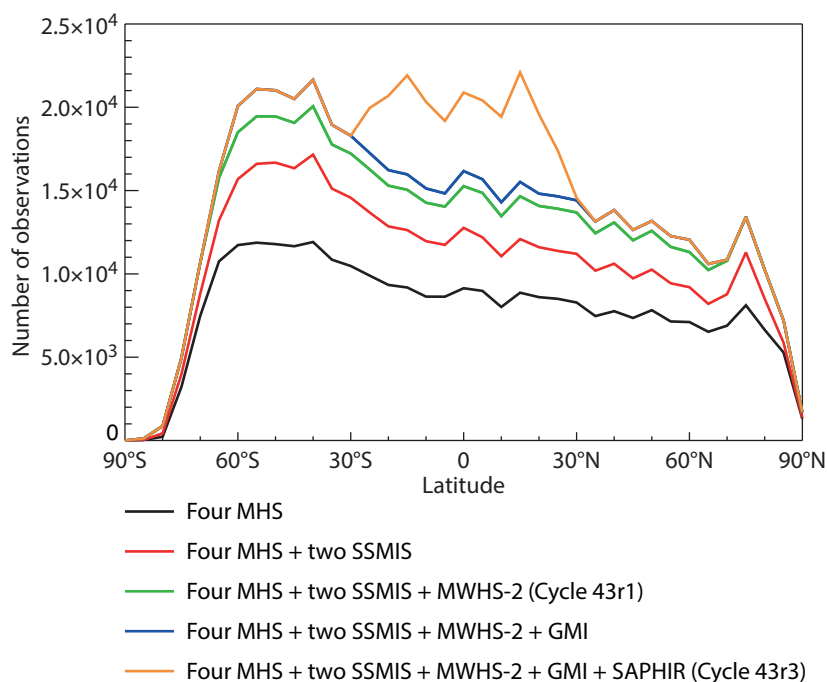


Figure 3 Number of assimilated all-sky microwave humidity observations around 183.3 ± 3 GHz as a function of latitude for 31 August 2016. The number of observations used in Cycle 43r1 is shown in green, with contributions from four microwave humidity sounders (MHS), two Special Sensor Microwave Imager/Sounders (SSMIS) and one Micro-Wave Humidity Sounder 2 (MWHS-2) instrument. In Cycle 43r3, observations from the Global Precipitation Measurement Microwave Imager (GMI) and the Sounder for Atmospheric Profiling of Humidity in the Inter-tropical Regions (SAPHIR) have been added.

filter. A positive side effect of this change is a reduction of around 5% in the time spent in the critical path of 4DVAR. Figure 2 shows the impact of these changes on the analysis of tropical cyclone Patricia (23 October 2015, Eastern Pacific).

Observations

Cycle 43r3 makes greater use of microwave sounding data by adding new sensors and improving the usage of existing data. The Global Precipitation Measurement Microwave Imager (GMI) humidity-sounding channels have been activated along with SAPHIR (Sounder for Atmospheric Profiling of Humidity in the Inter-tropical Regions), a humidity sounder with frequent tropical coverage (Figure 3). Microwave Humidity Sounder (MHS) observation errors have been reduced over land, and MHS channel 4 is now used over snow-covered land surfaces. Additional Advanced Technology Microwave Sounder (ATMS) humidity and temperature sounding channels are being used over sea ice and cold seas. The Micro-Wave Humidity Sounder 2 (MWHS-2) 118 GHz channels, which are sensitive to temperature and cloud, have been added over land surfaces. There have also been passive updates to prepare for the all-sky assimilation of the Advanced Microwave Sounding Unit-A (AMSU-A), and possible future use of the Micro-Wave Radiation Imager (MWRI). These changes increase the existing impact of all-sky humidity observations. The largest improvements are seen for vector wind and of course humidity itself. Anomalously high atmospheric concentrations of hydrogen cyanide (HCN) from wildfires are now detected dynamically and infrared observations are only excluded when safe thresholds are exceeded. This replaces the previous approach of constantly blacklisting all potentially HCN-affected channels. The first-guess check for radio occultation observations has been tightened. The radiosonde vertical consistency check has been relaxed and observation errors for temperature and humidity now depend on radiosonde type.

Convection scheme changes

Several improvements in the treatment of microphysical processes in the convection scheme affect the profile of latent heat release. In particular:

- Glaciation of cloud water now occurs in the temperature interval from 0 to -38°C rather than 0 to -23°C , with freezing rain treated directly in the updraft scheme.
- Snow now melts to form rain when wet-bulb rather than dry-bulb temperature is 0°C .
- Not just cloud condensate but also rain and snow are now detrained to the cloud scheme.

Temperature and geopotential-height biases at the melting level and in the upper troposphere have been strongly reduced. Tropospheric winds in summer, notably subtropical jets, have strongly improved. A measureable improvement in forecast skill is evident in the northern-hemisphere summer. Elsewhere the impact is mostly neutral.

New radiation scheme

The radiation scheme has been completely recoded to be much more flexible. The four primary components (gas optics, cloud optics, aerosol optics and solver) can now be changed independently of each other, and it is possible to choose between several new solvers that include longwave scattering and three-dimensional radiative effects. The first operational implementation in 43r3 is similar to the old radiation scheme, but there are already three improvements. First, the new scheme is 30–35% faster than the old one. Second, thanks to a more exact solution of the longwave equations, extreme values in the temperature profile are reduced, which means that the tropopause is now warmer and the stratopause is now cooler in the model, reducing the existing bias in both locations (Figure 4). Third, the new McICA scheme to represent cloud structure is less noisy in partially cloudy situations, which leads to a small improvement in tropospheric forecast skill

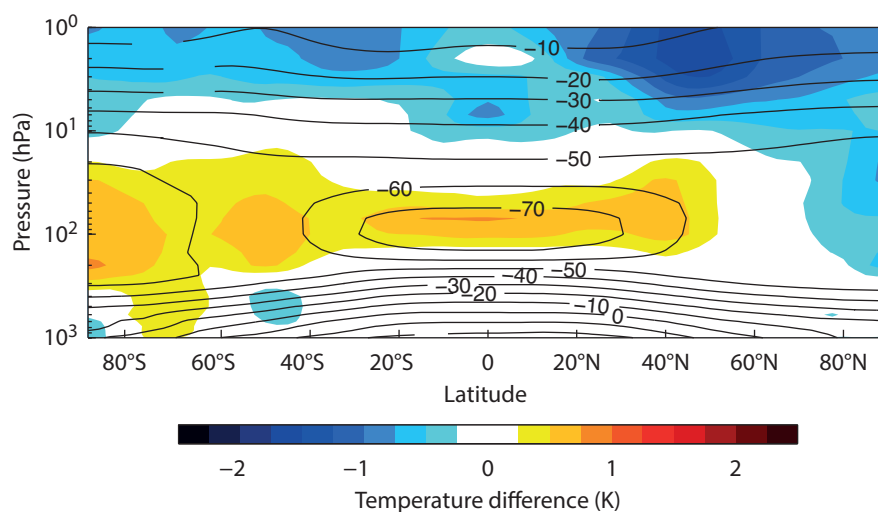


Figure 4 Difference in zonal-mean temperature between the new radiation scheme and the previous one (IFS Cycle 43r3 minus IFS Cycle 43r1 – shading) for a four-year coupled climate simulation. The contours show temperature in $^{\circ}\text{C}$ according to the climate simulation using IFS Cycle 43r3. The upgrade reduces the existing bias in the tropopause and the stratopause.

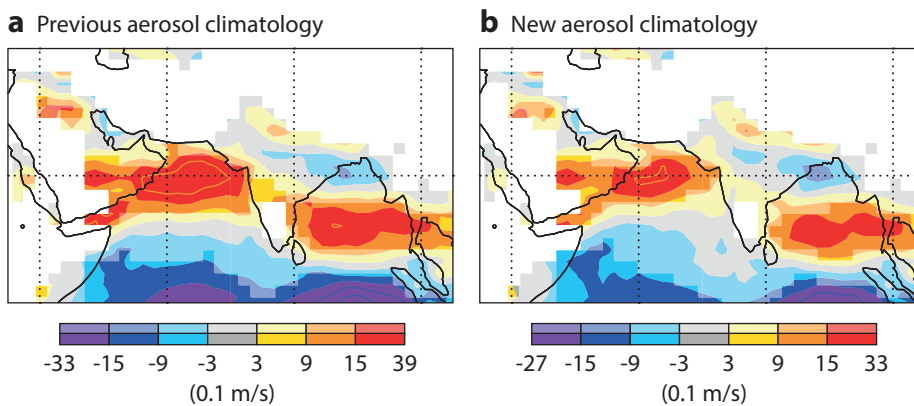


Figure 5 Bias in the day-5 forecast of 925 hPa zonal wind in the Indian monsoon region in summer (June–August) for (a) the previous IFS cycle, 43r1, and (b) IFS Cycle 43r3 with the new aerosol climatology. Saturated colours indicate areas where the signal is significant at the 95% confidence level.

(smaller than that brought about by the changes to the convection scheme).

New aerosol climatology

In Cycle 43r3, the Tegen aerosol climatology, which was operational for 14 years, has been replaced with a new climatology derived from data provided by CAMS. This includes the rigorous computation of aerosol optical properties using revised refractive indices in each band of the entire longwave and shortwave spectrum. In addition, the humidification of hydrophilic aerosol is modelled by exploiting the dependence of optical properties on relative humidity. The new climatology leads to an improved representation of the Indian summer monsoon, which is currently too strong in the IFS (Figure 5). A reduction in the absorption of shortwave radiation over Arabia leads to less solar heating and hence a reduction in the strength of the Arabian heat low. This in turn reduces the bias in westerly wind into India by around 25%, which halves the current overestimate of rainfall over the west coast of India.

Software infrastructure

As part of the upgrade, IFS version control has been migrated from the Perforce version to Git, and the JIRA tool has been introduced for issue tracking and software management (see the separate article on these developments in this issue of the Newsletter). In addition, changes have been introduced to make it possible to perform single-precision experiments for all applications. Running parts of the IFS at single precision (with a 32-bit representation of real numbers) instead of double precision (a 64-bit representation of real numbers) has the potential to dramatically increase computational efficiency without compromising forecast quality. It could

lead to more efficient experimentation and possibly even forecast production. This is an area of active research (Váňa *et al.*, 2016).

Summary

The ten-year Strategy adopted by ECMWF in 2016 includes two key scientific goals to help achieve improved medium-range forecast skill: a more accurate estimation of the initial state and the consistent representation of uncertainty associated with observations and the model; and a better representation of physical and chemical processes and of the interactions between different Earth system components. This IFS upgrade brings important advances in both areas. It enables the use of more observations and improves their assimilation; and it includes changes to the convection and radiation schemes and introduces a new aerosol climatology, thus bringing an improved representation of Earth system processes. Both developments have led to significant improvements in forecast skill. The upgrade also helps to pave the way for future progress by updating ECMWF’s software infrastructure. This will notably facilitate further work on single precision, which is expected to make an important contribution to the Centre’s Scalability Programme.

FURTHER READING

Buizza, R., J.-R. Bidlot, M. Janousek, S. Keeley, K. Mogensen & D. Richardson, 2017: New IFS cycle brings sea-ice coupling and higher ocean resolution, *ECMWF Newsletter No. 150*, 14–17.

Váňa, F., G. Carver, S. Lang, M. Leutbecher, D. Salmond, P. Düben & T. Palmer, 2016: Single-precision IFS, *ECMWF Newsletter No. 148*, 20–23.

doi:10.21957/yp392k

Monitoring thin sea ice in the Arctic

STEFFEN TIETSCHKE,
MAGDALENA BALMASEDA, HAO ZUO

As part of the new OCEAN5 high-resolution ocean/sea-ice model and data assimilation suite, which was implemented in November 2016, ECMWF now routinely obtains and processes a sea-ice thickness product for thicknesses of up to about 1 metre from the University of Hamburg. This innovative observational product can help ECMWF to improve the representation of Earth system interactions in the Integrated Forecasting System (IFS), in line with the emphasis on Earth system modelling in the Centre's new ten-year Strategy.

The product is based on satellite observations of brightness temperatures from the European Space Agency's SMOS mission. The sea-ice thickness data derived from it can be compared to the sea-ice analysis produced by OCEAN5, which does not yet assimilate sea-ice thickness observations. This comparison helps to evaluate the performance of OCEAN5 on the one hand and to assess the information content and uncertainties of the observations on the other. First evaluation results show encouraging similarities between observations and the OCEAN5 analysis although there are also some regional discrepancies.

Importance of sea-ice thickness

Sea-ice thickness is defined as the vertical distance from the air-ice interface at the top of the sea ice to the ice-water interface at the bottom of the sea ice. It has received far less attention in ECMWF's modelling and forecasting efforts than sea-ice concentration, which is the fraction of a given ocean area that is covered by sea ice. Current operational systems like the high-resolution forecast (HRES) and the 4DVAR analysis use observed sea-ice concentration but assume a constant sea-ice thickness of 1.5 m. In reality, any thickness from a few centimetres to more than 5 metres is possible. This results in very different surface heat fluxes especially in winter, when the temperature contrast between the surface atmosphere and the ocean water below the sea ice can be as large as 40 K. Moreover, sea-ice thickness is indispensable for predicting the evolution of sea-ice cover days to months ahead: thin ice will evolve much more quickly than thick ice because it is more susceptible to dispersion or compression by winds. In addition, by allowing larger surface heat fluxes it can lose or gain mass much faster than thick ice. Small differences in the ice thickness at the beginning of summer can also make a large difference to the timing of its complete disappearance during the melt season, which in turn causes large differences in the forecast air temperature near the surface.

Despite the importance of sea-ice thickness for medium-range to seasonal predictions, two factors have prevented its explicit treatment until recently: the lack of a prognostic sea-ice model in the ECMWF forecasting systems and the

scarcity of observations. The first obstacle was overcome in November 2016 with the implementation of OCEAN5 as part of an upgrade of ECMWF's Integrated Forecasting System (IFS Cycle 43r1). For the first time, the IFS now contains a fully prognostic sea-ice model, the Louvain-la-Neuve Sea Ice Model version 2 (LIM2) developed at the Belgian Université catholique de Louvain. This is used to produce physically-based analyses and forecasts of sea-ice thickness. The second obstacle, the lack of observations with sufficient spatial and temporal coverage, has diminished with the arrival of novel satellite observations over the past ten years.

New observations

Two types of satellite observations have recently made it possible to go beyond the sparse observations of sea-ice thickness from field campaigns and autonomous ice-tethered buoys that have been available for many years. First, high-resolution altimetry data from the ICESat and CryoSat2 missions have made it possible to directly measure the freeboard of sea ice (the vertical distance from the top surface of sea ice to adjacent water surfaces). From this its thickness can be derived. Second, the Aquarius, SMOS and SMAP missions have started to observe the radiance of the Earth's surface in the L-band frequency of 1.4 GHz. Emissivity at this frequency varies with sea-ice thickness. While altimeter measurements only work for thick ice (more than about 0.5 m), L-band radiances are only sensitive to differences in the thickness of sea ice which is less than about 1 m thick. Thus the two methods complement each other well, and the full range of sea-ice thickness can in principle be observed by combining them.

In the remainder of this article, we discuss ice thickness derived from L-band (1.4 GHz) observations made by the SMOS satellite (Box A) and how it compares to ice thickness in the OCEAN5 analysis. Figure 1 shows a recent example of daily-mean L-band brightness temperatures (T_B) from SMOS together with the sea-ice thickness from the Hamburg product (SMOS-SIT) derived from them. For reference, the sea-ice concentration from the OSTIA product for the same day is also shown. Although the sea-ice concentration is close to 100% throughout the interior of the ice pack, the ice thickness as derived from SMOS T_B is far from uniform. There is, for example, an extended zone of thin sea ice along the Siberian coast, where ice has been pushed offshore by the winds and the resulting open-water area has subsequently refrozen. These features within the ice pack are called coastal polynyas. They occur frequently throughout the Arctic winter. In the Beaufort Sea north of Alaska, a large fracture zone is visible with many individual, curved cracks. These cracks are the result of shear arising from the rotation of sea ice in a gyre forced by the prevailing wind patterns. Importantly, polynyas and fracture zones in winter often refreeze so quickly that they seem continuously ice-covered. They are therefore hard to detect from observations of passive microwave

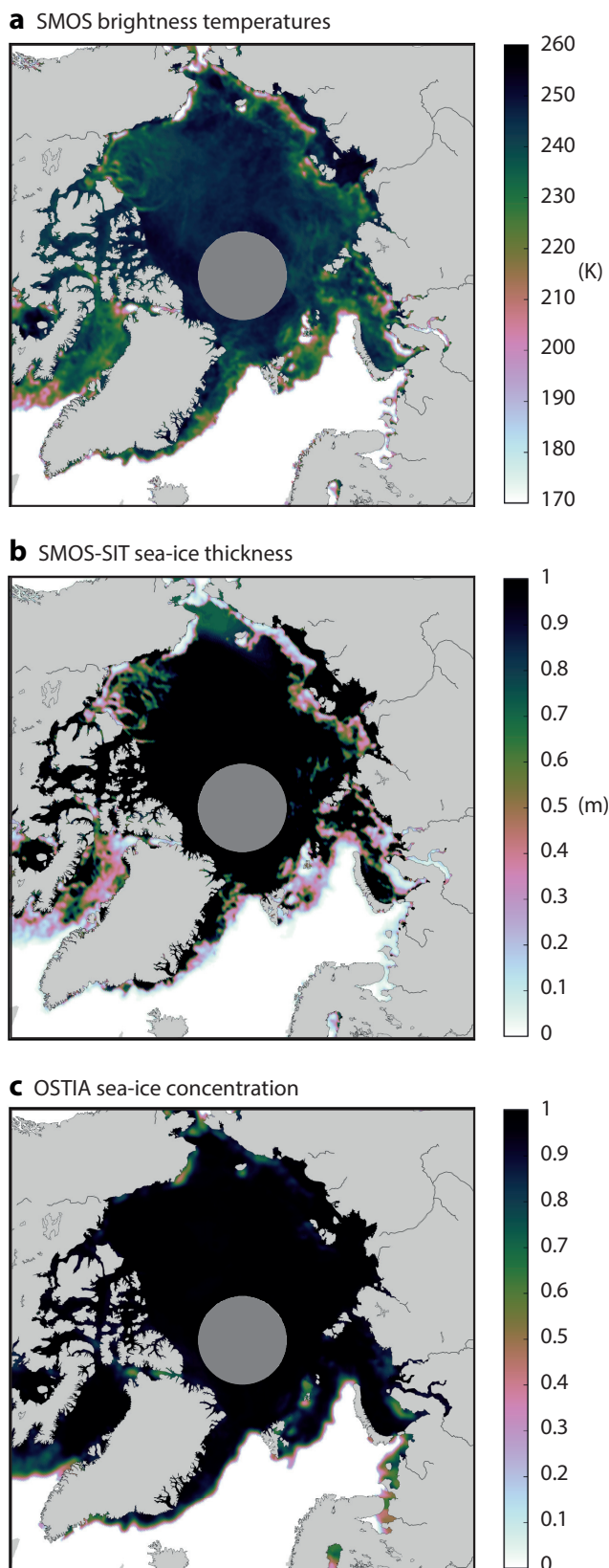


Figure 1 Daily-mean fields for 16 April 2017 showing (a) brightness temperature from SMOS, (b) sea-ice thickness from the SMOS SIT product, and (c) OSTIA sea-ice concentration. The area around the North Pole is greyed out because of a lack of satellite observations in this region.

radiation with shorter wavelengths that originates from near the surface of the ice. However, Figure 1 shows clearly that SMOS T_B is sensitive to these features: the derived ice thickness is often below 0.5 m here, whereas outside these features it is in excess of 1 m. Heat conduction through the newly formed sea ice can be substantial: an approximate calculation shows that the surface heat flux over some of the thin-ice regions was of the order of 100 W m^{-2} .

Uncertainties and biases

While this example demonstrates the additional value of L-band ice thickness observations, the question is how to make best use of the information contained in these observations. This requires a critical assessment of uncertainties and biases in both observations and the model. On the one hand, uncertainties in L-band sea-ice thickness are not small: as indicated in Box A, the thermodynamic and radiative transfer modelling that is required to derive sea-ice thickness from L-band brightness temperature is complex. It is sensitive to other co-located meteorological and oceanographic parameters, which themselves contain considerable uncertainties, and it

Sea-ice thickness from SMOS

A

The sea-ice thickness product provided by the University of Hamburg (SMOS-SIT) contains Arctic-wide daily means with 12.5 km nominal resolution. It is provided with a delay of less than 24 hours for the duration of the freezing period from mid-October to mid-April. The retrieval method makes it possible to measure the thickness of thin young ice up to a thickness of 1 m.

The retrieval algorithm of the University of Hamburg group (Tian-Kunze et al., 2014) is applied to L-band (1.4 GHz) brightness temperatures (T_B) provided by the SMOS satellite, and it also works well for T_B provided by SMAP. The algorithm is based on the radiation intensity (average of horizontal and vertical polarisation), which is robust against instrumental and geophysical errors and relatively independent of incidence angle. The L-band wavelength of 21 cm is large compared to typical inhomogeneities in the ice in the vertical, and is of the same order as the ice thickness to be measured. Therefore, the expected emissivity from a slab of sea ice with sea water underneath can be calculated based only on the thickness d of the slab and its dielectric properties. The dielectric properties mainly depend on the bulk temperature and salinity of the sea ice, which are derived from ancillary fields and a simple thermodynamic model. The ancillary fields are mainly 2 m air temperature T_{air} from an atmospheric (re-)analysis and the ocean surface salinity S from an ocean model simulation. Given the observed brightness temperature T_B , the retrieved ice thickness d is then found by iteratively solving the equation $T_B = f(d, T_{air}, S)$, where the forward model f contains both the translation of the ancillary fields into the sea ice bulk properties and the radiative transfer model that calculates the emissivity. The retrieval works well when the sensitivity of T_B to changes in ice thickness is larger than its sensitivity to bulk temperature and salinity.

relies on several simplifying assumptions which are not always valid. On the other hand, OCEAN5 has a simplified representation of thin sea ice, and its data assimilation scheme does not properly account for error covariance between sea ice concentration and thickness.

A quite stringent comparison between ice thickness estimates from SMOS SIT and OCEAN5 is provided by the joint frequency distribution of co-located observations and model equivalents shown in Figure 2. It has been calculated for all days during the winter 2016/17 and at all locations where the diagnostic uncertainty parameters provided with SMOS-SIT suggest that the observational estimate should be reliable. There is a degree of correspondence between observed and analysed ice thickness, but there are also some major discrepancies. Most notable is the tendency for OCEAN5 to have greater ice thickness than SMOS-SIT, with a considerable amount of spread. For instance, the model equivalent of the SMOS-SIT thickness range 0.4–0.6 m has a wide distribution with a maximum between 0.6–0.9 m and frequently occurring ice thicknesses of up to 1.5 m. Decomposing this signal into different regions and months reveals a complex picture: independent data suggests that the true thickness is closer to the SMOS-SIT data in some cases, but closer to the OCEAN5 analysis in others (Tietsche et al., 2017). SMOS-SIT data tend to be better in the recently refrozen fracture zones and polynyas shown in Figure 1, which are often poorly represented in the model. The model seems to perform better in some specific regions, such as the Labrador Sea: as shown in Figure 1, SMOS-SIT detects thin sea ice there, whereas OCEAN5 and altimeter data suggest the presence of thick

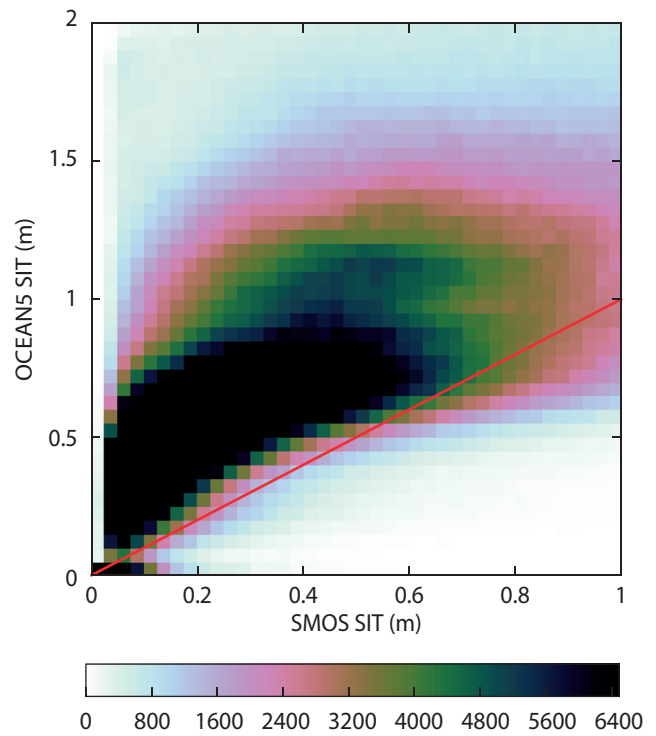


Figure 2 Scatter density plot showing the number of data points in each bin for daily co-located sea-ice thickness up to 1 m from the SMOS-SIT product and its OCEAN5 model equivalent from mid-October 2016 to mid-April 2017. Only those data points of SMOS-SIT are considered where the uncertainty diagnostics provided with the dataset indicate a reliable retrieval.

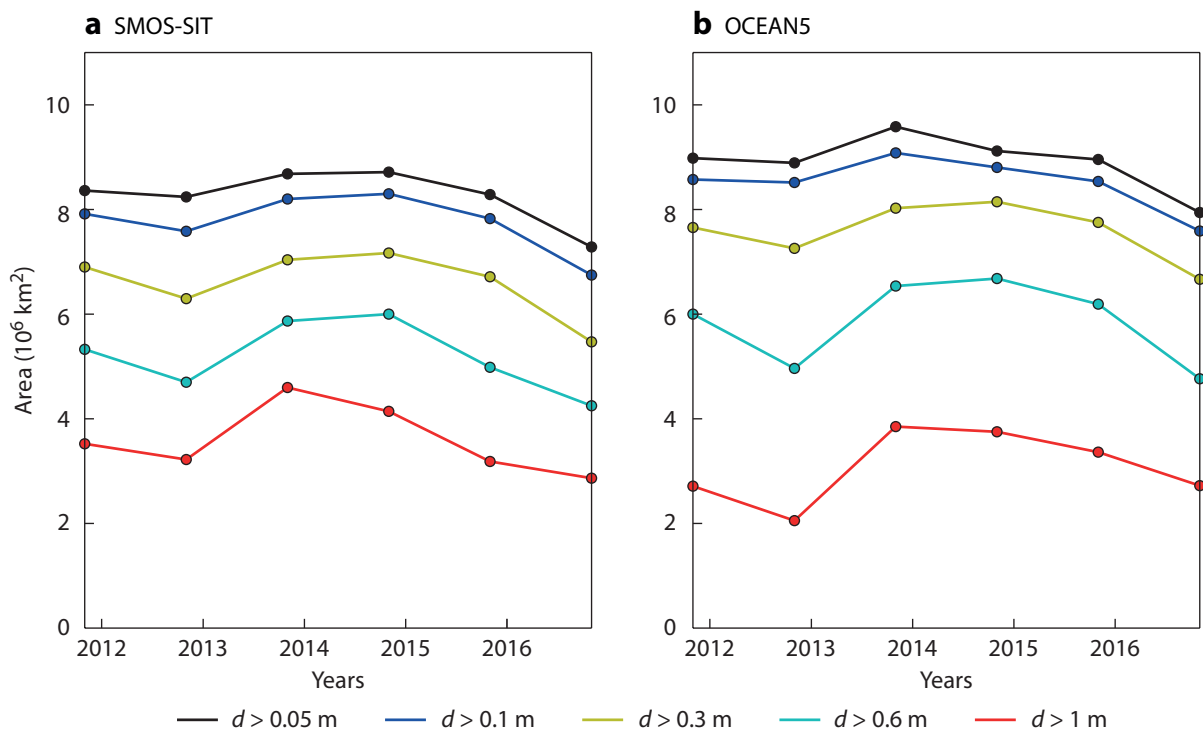


Figure 3 Area which is covered by sea ice exceeding various thickness thresholds in November for the years 2011 to 2016, showing (a) the area as derived from the SMOS-SIT observational product and (b) the area as derived from the OCEAN5 analysis.

ice. It should be noted that agreement between the model and observations is generally quite good early in the freezing season, and throughout the freezing season in the Barents Sea. The agreement tends to deteriorate later in the freezing season, especially for regions with frequent polynyas and in the Labrador Sea.

Despite these uncertainties at a regional scale, there is good agreement in the large-scale distribution and interannual variability of thin sea ice. Figure 3 shows time series of the area covered by sea ice with thicknesses above various thresholds in November in the years 2011 to 2016. The uppermost curve is the area of sea ice which is at least 5 cm thick; it corresponds quite well to the sea-ice extent given by the US National Snow and Ice Data Center (NSIDC) if the observational gap around the North Pole is taken into account. The lowermost curve is the area of sea ice which is more than 1 m thick. There is generally good agreement between the magnitude, variability and trend of the areas of the various thickness classes as simulated by OCEAN5 and as derived from SMOS observations. The extreme summer minimum in 2012 left that year's November with markedly reduced sea-ice area for all thickness classes. In 2013, there was a clear recovery. Since then, there has been a downward trend in all classes. Figure 3 demonstrates that both OCEAN5 and SMOS-SIT capture important year-to-year variability and trends in the state of Arctic sea ice even though the OCEAN5 analysis does not use SMOS-SIT and is therefore independent of it.

Conclusion

Sea-ice thickness observations from L-band radiometry are a novel and innovative technology with great

potential. We are only just beginning to harness it. It needs to be borne in mind that it is fundamentally limited to thin sea ice, and much more research is needed into its sensitivities to ancillary data and the assumptions in the complex physically-based retrieval model. At the same time, prognostic sea-ice modelling at ECMWF has been operational for less than a year, and many modelling and data assimilation improvements are imminent. In this light, the results presented here are encouraging. To make progress in better characterising the uncertainties in the data, it would be beneficial to integrate the retrieval model into the ECMWF system, i.e. to use the meteorological and oceanographic surface fields coming from the ECMWF atmosphere and ocean analyses to feed the retrieval model. The next step would be the development of stable and reliable multivariate sea-ice data assimilation schemes which can fully exploit the sea-ice thickness information provided by L-band radiometry to arrive at an improved sea-ice analysis. These steps will provide important building blocks in efforts to improve predictions in the polar regions.

FURTHER READING

Tietsche, S., M. Balmaseda, H. Zuo & P. de Rosnay, 2017: Comparing Arctic winter sea-ice thickness from SMOS and ORASS, *ECMWF Technical Memorandum No. 803*.

Tian-Kunze, X., L. Kaleschke, N. Maaß, M. Mäkynen, N. Serra, M. Drusch, & T. Krumpfen, 2014: SMOS-derived thin sea ice thickness: algorithm baseline, product specifications and initial verification. *The Cryosphere*, **8**, 997–1018.

doi:10.21957/51j3sa

Assessing the impact of observations using observation-minus-forecast residuals

MOHAMED DAHOUI, LARS ISAKSEN, GABOR RADNOTI

ECMWF assimilates a wide range of observations to help define the initial conditions at the start of a forecast run. It uses a complex data assimilation scheme (4DVAR) to make the best possible use of the available observations. Given the importance of accurate initial conditions for the quality of forecasts, it is useful to monitor and understand the relative impacts of different parts of the observing system on the analysis as well as on forecasts. ECMWF routinely assesses Forecast Sensitivity to Observation Impact (FSOI) using an 'adjoint-based' approach where forecast skill is evaluated with respect to analyses. An alternative, observation-based measure of impact called 'observation-minus-forecast (OMF) residuals' has been implemented and found to provide complementary results. Results using the OMF residuals approach differ from FSOI but confirm the strong influence of satellite observations, which dominate the observing system in terms of volume. Both measures show that in-situ measurements remain an essential component of the observing system despite their relatively low numbers compared to satellite observations.

The overall impact of observations on the analysis and on forecasts depends on the quality of the assimilation system and the forecasting model and locally on the characteristics of the Earth's surface and dominant weather regimes. The relative impact of each component of the observing system depends on its quality, spatial and temporal distribution, prescribed observation errors (derived from a long-term statistical evaluation of the observing system) and inherent redundancies with other components of the observing system. To estimate the impact of observations, different methods are used. The results obtained depend on the verification measures employed and the atmospheric structures targeted.

Observation impact methods

Data denial experiments (generally referred to as Observing System Experiments or OSEs) are the most appropriate method to quantify the impact of individual components of the observing system. They are systematically performed before actively assimilating new observation types. Occasionally data denial experiments are conducted to help ECMWF and data providers optimise the assimilation system or to give valuable information about current observing systems and guidance for future observing systems. However, OSEs are expensive because they necessitate additional long-term data assimilation and forecast experiments, denying each observing system under investigation one by one. This cannot be done frequently to evaluate the many different components of the observing system. OSEs are therefore not suitable for day-to-day monitoring. Efficient and less expensive complementary tools have been developed for that purpose.

So-called 'adjoint-based' approaches offer a powerful complement to OSEs by estimating the contribution of different types of observations to the increase or decrease in forecast error. These methods identify the relationship between the short-range forecast error (evaluated against the analysis) and the observations used in the assimilation (Box A). An adjoint-based FSOI system was implemented operationally at ECMWF in June 2012 and is run every day to continually produce estimates of observation impact (*Cardinali, 2009*).

Todling (2012) suggested another approach to estimate observation impact by making use of differences between observation-minus-forecast residuals (OMF residuals) obtained from consecutive forecasts (Box B). This approach is simpler and less costly than FSOI but it assumes a high degree of temporal homogeneity in the observing system. *Liu & Kalnay (2008)* have proposed an ensemble-based observation impact estimation technique that does not require the use of forecast model and data assimilation adjoints. This approach is not discussed in this article but will be explored in the future, using the EDA (Ensemble of Data Assimilations).

Limitations

Observation impact methods are based on assumptions and approximations that need to be taken into account when interpreting the results. The main considerations for the adjoint-based approach using the analysis as the verification state are that:

- Errors in the analysis can mask the impact of observations. In extreme cases, such errors are incorrectly interpreted as a negative impact of observations.
- The verification state should ideally be uncorrelated with the forecast. This is not the case when the analysis is used.
- Different choices of forecast error measure (the 'norm') can be made and this fundamentally affects the resulting estimates of observation impact.
- The adjoint-based method is restricted by the use of a linearised version of the model, which makes it valid only to evaluate short-range forecasts (0 to 48 hours).
- Biases in the model (compared to the analysis) may erroneously be interpreted as a negative impact of observations, where they really represent model errors.

The main considerations for OMF residuals are that:

- The method captures only part of the forecast error (the part projected onto the space of observations) and the choice of norm is very limited.
- The method assumes sufficient homogeneity of the observing system between the initial time and the verification time. Such an assumption means that any

conclusions regarding observation impact should be based on statistics and cannot be applied to individual cases or individual stations.

- Since some observations are bias-corrected, there is an undesirable correlation between the forecast and the verification.

Observation impact results

In order to compare the results from OMF residuals and adjoint-based approaches, we accumulated statistics for a three-week period. For the adjoint-based approach, we used operationally produced FSOI statistics (based on IFS Cycle 43r1, operational since November 2016). Statistics from the OMF residuals approach were derived from an experiment run at the operational resolution (IFS Cycle 43r1). Figure 1 shows the relative 24-hour observation impact per data type derived from the operational adjoint-based approach and the OMF residuals. Statistics cover the period from 6 to 28 November 2016. ACARS (Aircraft Communications Addressing and Reporting System) data have greater impact according to the

OMF residuals method than they do according to the adjoint-based approach, likely because reduced impact from data redundancy for dense aircraft data over the USA is handled better by FSOI. The two hyper-spectral instruments CrIS and IASI appear to have more estimated impact using the OMF residuals method. For these two instruments overcast observations (completely cloudy scenes) are used in the analysis. In a small number of cases the forecast departures have very large negative values, which indicates a significant mismatch of cloudiness between the forecast and these overcast pixels. When these cases are detected the inter-channel correlation of observation errors are partially ignored in the computation of observation impact to avoid affecting the results for other channels. GPS radio occultation (GPSRO), atmospheric motion vectors (SATOB), scatterometers (SCATT), radiosondes (TEMP) and buoys (DRIBU) appear to have less impact according to the OMF residual measure. Due to a temporary outage of data from two key satellites (Metop-B and AQUA), the impact of AMSU-A (Advanced Microwave Sounding Unit-A)

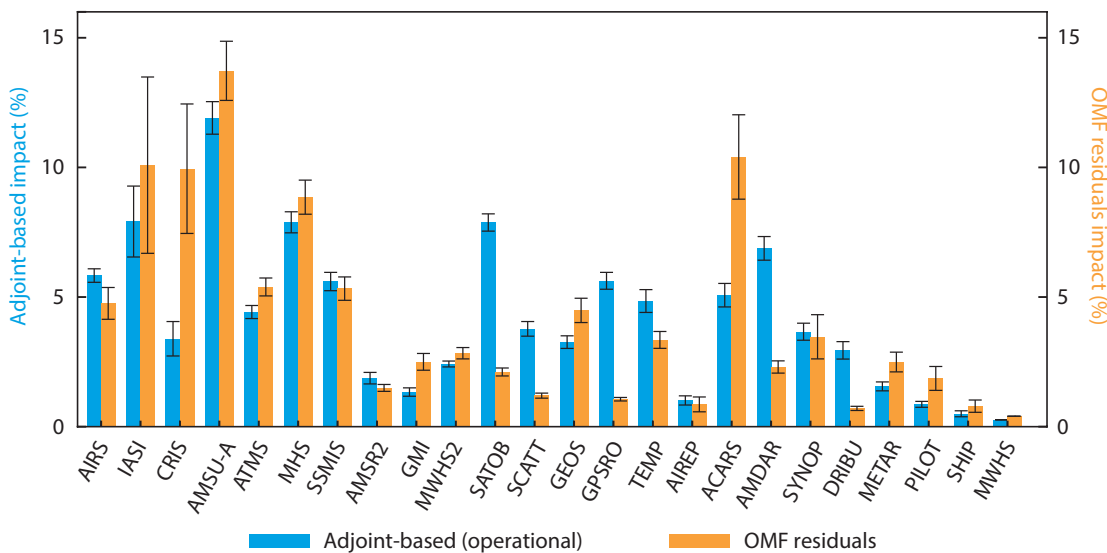


Figure 1 Relative 24-hour observation impact per data type, obtained using the operational adjoint-based approach and OMF residuals. Statistics cover the period from 6 to 28 November 2016. The error bars are computed using the day-to-day variability of the mean relative impact. For an explanation of the acronyms, see Table 1.

AIRS	Atmospheric Infrared Sounder	AMSR2	Advanced Microwave Scanning Radiometer 2	AIREP	Aircraft reports
IASI	Infrared Atmospheric Sounding Interferometer	GMI	Global Precipitation Measurement (GPM) Microwave Imager	ACARS	Aircraft Communications Addressing and Reporting System
CRIS	Cross-track Infrared Sounder	MWHS2	MicroWave Humidity Sounder 2	AMDAR	Aircraft Meteorological Data Relay
AMSU-A	Advanced Microwave Sounding Unit-A	SATOB	Atmospheric motion vectors	SYNOP	SYNOP network weather stations
ATMS	Advanced Technology Microwave Sounder	SCATT	Scatterometer	DRIBU	Buoys
MHS	Microwave Humidity Sounder	GEOS	Geostationary Operational Environmental Satellite system	METAR	Weather reports from airports
SSMIS	Special Sensor Microwave Imager/Sounder	GPSRO	GPS radio occultation	PILOT	Wind observations from PILOT radiosondes and radar profilers
		TEMP	Radiosondes	SHIP	Ship-based instruments
				MWHS	MicroWave Humidity Sounder

Table 1 Components of the global observing system.

A

Adjoint-based observation impact technique

Langland & Baker (2004) introduced an adjoint-based approach to estimate the impact of observations on short-range forecasts (the adjoint is a matrix transpose which back-projects information from data to the underlying model). In the adjoint-based approach, a forecast error measure is defined involving the comparison of the forecasts against a proxy of the true state. The change in this error measure, computed for forecasts valid at the same time issued from two consecutive analyses, is solely due to the assimilated observations. Using the adjoint of the model and the analysis, one can relate the change in the forecast error to assimilated observations. The forecast error measure e_f is defined as:

$$e_f = (\mathbf{x}_k^f - \mathbf{x}^t)^T \mathbf{C}(\mathbf{x}_k^f - \mathbf{x}^t)$$

Where \mathbf{x}_k^f and \mathbf{x}^t are the predicted (from initial time k) and true states, respectively. \mathbf{C} is a weight applied to the forecast error. Consider forecasts from the analysis \mathbf{x}_a and the background \mathbf{x}_b , which is a short-range forecast based on the previous analysis. The difference $\delta e_f = e_{f(a)} - e_{f(b)}$ measures the combined impact of all observations assimilated. It can be estimated as a sum of contributions from individual observations using information from the model and analysis adjoints. Approximations of the variation in e due to variations in \mathbf{x}_a and \mathbf{x}_b are given by the Taylor series with various orders of approximation. The second order approximation used in the ECMWF FSOI implementation (Cardinali, 2009) is:

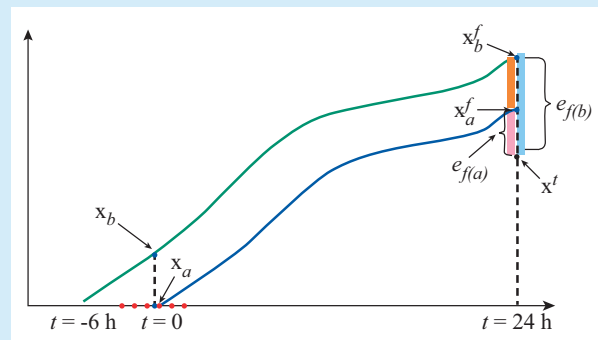
$$\delta e = (\mathbf{y} - \mathbf{h}(\mathbf{x}_b))^T \mathbf{K}^T [\mathbf{M}_b^T \mathbf{C}(\mathbf{x}_a^f - \mathbf{x}^t) + \mathbf{M}_a^T \mathbf{C}(\mathbf{x}_b^f - \mathbf{x}^t)]$$

where \mathbf{y} is the observation vector, \mathbf{h} is the observation operator transforming model values into observation-like values, \mathbf{K}^T is the adjoint of the analysis, and \mathbf{M}_a^T and \mathbf{M}_b^T are the matrices of the model adjoint based on trajectories starting from the analysis and the background, respectively.

For any set of observations, $\delta e < 0$ represents a reduction in forecast error. $\delta e > 0$ means that the observations have caused an increase in forecast error.

Since the true state is unknown, the method uses the analysis or observations as a proxy of the truth. In the ECMWF implementation, the analysis is used. The error measure is computed globally and weighted using a dry energy norm. Other choices of the weight (norm) might lead to a different estimation of the impact (Todling, 2012) and therefore it is important to take this into account when interpreting impact results. The dry energy norm used at ECMWF gives more weight to tropospheric observations. With this method other bespoke norms can be adopted.

When observations are used as a proxy of the truth, the weight is the observation errors as used in 4DVAR. This variant of the adjoint-based approach has been tested at ECMWF but not yet implemented.



Schematic of forecast error measure. Adapted from Langland & Baker (2004).

satellite data is less important here than in previously documented results (Cardinali, 2009). As indicated by the small standard deviation bars in the data count (Figure 2), the observing system was stable throughout the period, which is important for the validity of results from the OMF residuals approach.

The differences between the two measures of impact are related to the nature of the forecast error measure (the applied norm, see Box A). The forecast error measure in the adjoint-based approach using the analysis for verification is more encompassing as it is computed in model space involving all grid points. In the OMF residuals approach the forecast error measure is computed against available observations, which means that non-observed parts of the atmosphere are not captured. The total dry energy norm applied in the adjoint-based approach has more weight in the troposphere and the lower stratosphere than the norm used in the OMF residuals approach. In the latter, the weight is based on observation errors used in the assimilation system. They are more uniform with height. The impact of the norm is clearly visible when comparing the relative impacts of observations per vertical level, as

shown in Figure 3 (for AMSU-A) and Figure 4 (for GPSRO). Here the impact for stratospheric observations is greater according to the OMF residuals measure than it is for the adjoint-based measure, and it is significantly smaller for tropospheric data. Looking at the average impact per individual observation (Figure 5), it is clear from both measures that in-situ observations have a greater impact per observation. Buoys, ships, SYNOP weather stations and AIREP aircraft reports have the greatest impact per observation. The average impact of buoys is the highest, but according to the OMF residuals method it is not significantly bigger than that of SYNOP reports. Impact results obtained using the OMF residuals approach are in agreement with previous results obtained at ECMWF using an alternative implementation of the adjoint-based method (verified against observations and weighted by observation errors).

Discussion

Adjoint-based approaches are well established to estimate the impact of observations on forecasts. Their main limitation is related to the verification state. When used as a reference,

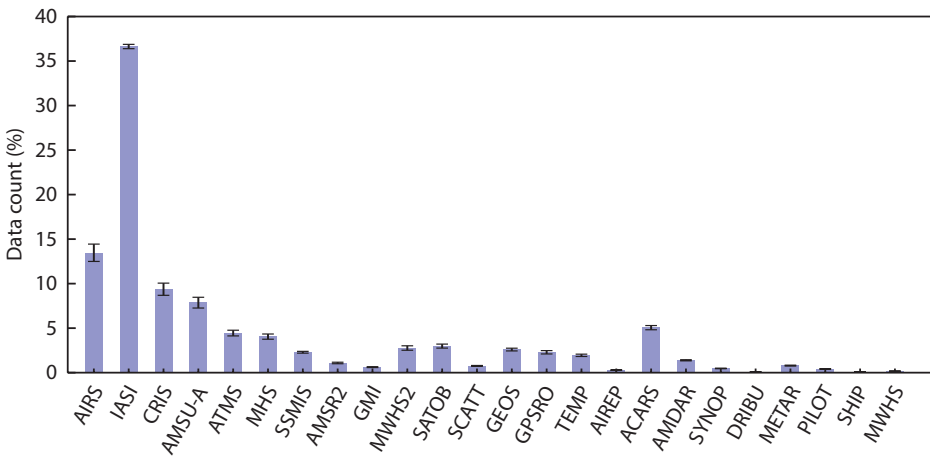


Figure 2 Relative data counts per data type. Statistics cover the period from 6 to 28 November 2016. The error bars are computed using the day-to-day variability of the mean relative data counts percentage.

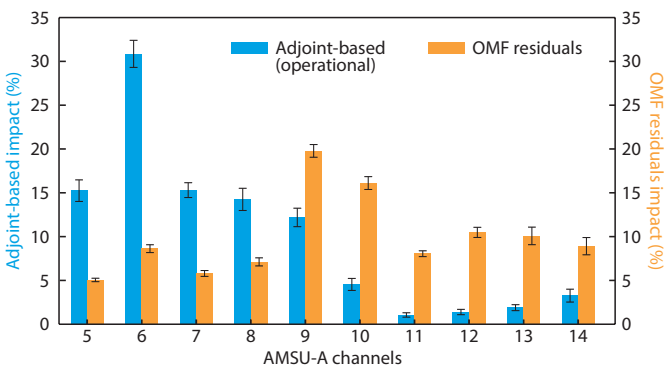


Figure 3 Relative 24-hour observation impact per AMSU-A channel, obtained using the operational adjoint-based approach and OMF residuals. Statistics cover the period from 6 to 28 November 2016. The differences between the results produced by the two methods can to a large extent be attributed to the different norms used: the dry energy norm applied in the adjoint-based approach has more weight in the troposphere and the lower stratosphere than the norm used in the OMF residuals approach.

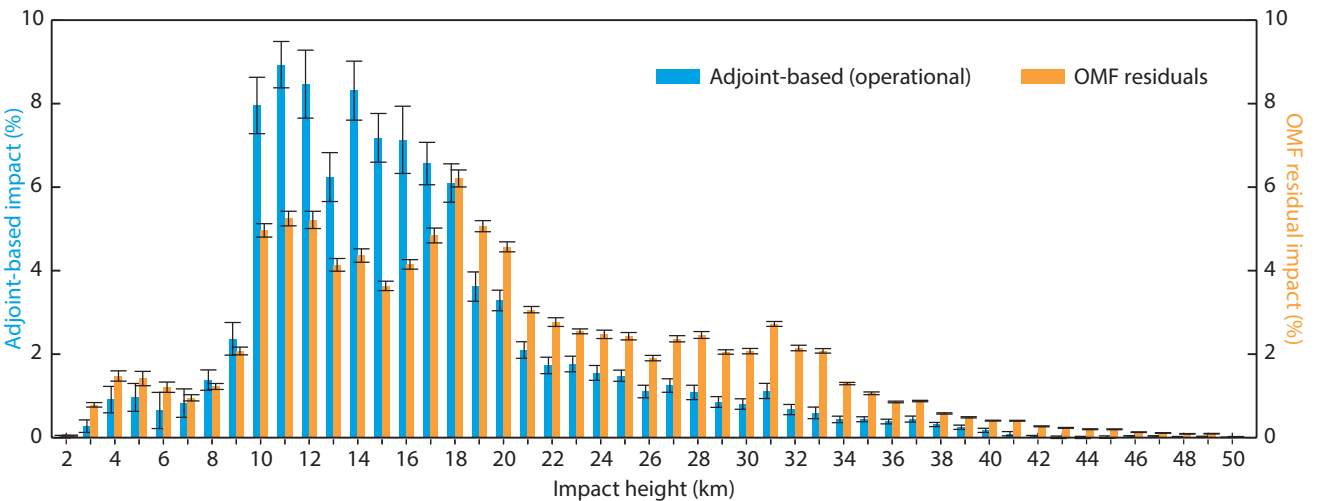


Figure 4 Relative 24-hour observation impact for GPSRO by impact height, obtained using the operational adjoint-based approach and OMF residuals. Statistics cover the period from 6 to 28 November 2016.

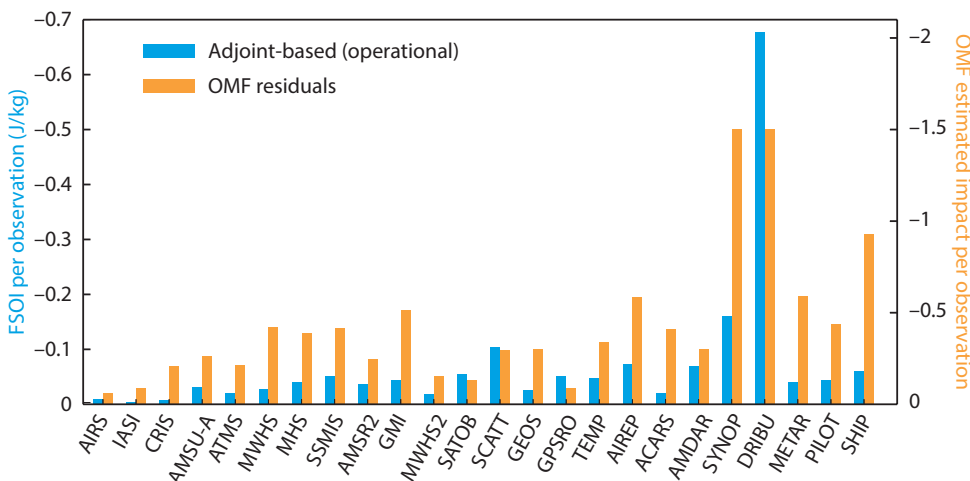


Figure 5 Average 24-hour contribution per observation report obtained using the operational adjoint-based approach and the OMF residuals. Statistics cover the period from 6 to 28 November 2016.

Observations impact using OMF residuals

Todling (2012) suggested a simpler and cheaper approach compared to FSOI for assessing observation impact using OMF residuals. The forecast error measure is computed using observations as a proxy of the truth. It is expressed as:

$$e_f^y = [\mathbf{h}(\mathbf{x}_{f|k}) - \mathbf{y}_f]^T \mathbf{C} [\mathbf{h}(\mathbf{x}_{f|k}) - \mathbf{y}_f]$$

where \mathbf{h} denotes the observation operator, $\mathbf{x}_{f|k}$ the forecast valid at the time f and issued from time k , \mathbf{y}_f represents verification observations at the time f , and \mathbf{C} is the inverse of the observation error variance. Similar to the adjoint-based approach, the forecast error reduction is determined by computing the difference between the error measures for forecasts valid at the same time issued from two consecutive analyses:

$$\delta e_f^y = e_{f|f-m+1}^y - e_{f|f-m}^y$$

where m is the forecast range.

The approach is based on the assumption that the observing system is sufficiently homogenous between the initial time

and the verification time for the partitioning of the impact into individual contributions from the various components of the observing system to be done at the verification time. Such an assumption is believed to allow a good projection (in a statistical sense) between the forecast error measure (computed by construction against observations at verification time) and the set of initial observations used. For this assumption to work the computation of the forecast error measure should involve only observations selected for use in the data assimilation (and not all available observations). Since the approach does not explicitly involve using the model adjoint, it can be applied to forecast ranges beyond the validity range of the model tangent linear. Applying the approach to step zero provides the impact of observations on the analysis. Observation impact results (fractional contribution) computed for the 24-hour forecast range can be compared to the operational adjoint-based FSOI.

OMF residuals are going to be computed routinely for all observations used operationally at ECMWF.

B

both the analysis and observations have limitations and it is advantageous to use both and to compare the results. ECMWF runs operationally an adjoint-based method using the analysis as the verification state. It is expected that in the near future the Centre will begin to routinely compute forecast departures in observation space to be used for verification. The availability of such forecast departures will make it easy and virtually cost-free to estimate observation impact in observation space. At least for short-range forecasts, the OMF residuals approach seems to provide sensible results that will complement the routinely produced FSOI statistics. The complementarity of the two approaches is mainly explained by their use of different verification references and choices of weight assigned to the forecast error measure.

Summary and prospects

For many years, ECMWF has been using an adjoint-based approach to estimate the impact of observations on forecasts. Although the method provides good guidance on the impact of observations, diagnostic activities will benefit from having access to complementary impact results based on observations as a proxy of the truth, and also using another error norm. The expected availability of observation-minus-

forecast (OMF) residuals will enable the routine, virtually cost-free computation of such additional diagnostics. The OMF residuals approach has the potential to be used for the estimation of observations impact at longer forecast ranges. This will be explored further and the results will be evaluated using the estimated impact of observations based on Observing System Experiments.

FURTHER READING

Cardinali, C., 2009: Monitoring the observation impact on the short-range forecast. *Q. J. R. Meteorol. Soc.*, **135**, 239–250.

Dahoui, M., G. Radnoti, S. Healy, L. Isaksen & T. Haiden, 2016: Use of forecast departures in verification against observations. *ECMWF Newsletter No. 149*, 30–33.

Langland, R. H. & N. Baker, 2004: Estimation of observation impact using the NRL atmospheric variational data assimilation adjoint system. *Tellus*, **56A**, 189–201.

Liu, J. & E. Kalnay, 2008: Estimating observation impact without adjoint model in an ensemble Kalman filter. *Q. J. R. Meteorol. Soc.*, **134**, 1327–1335.

Todling, R., 2012: Comparing two approaches for assessing observations impact. *Monthly Weather Review*, **141**, 1484–1505.

Calibrating forecasts of heavy precipitation in river catchments

AMARILLA MÁTRAI (General Directorate of Water Management, Hungary),
ISTVÁN IHÁSZ (Hungarian Meteorological Service)

Ensemble forecasts of severe weather can provide valuable information on the range of possible scenarios and the likelihood of their occurrence. However, to make sure ensemble forecasts are reliable, they need to be well calibrated. We have used a re-forecast-based method called quantile mapping to calibrate ECMWF ensemble forecasts (ENS) of precipitation. High-quality forecasts of heavy precipitation can assist hydrologists in their decision-making. We have therefore investigated re-forecast-based ensemble calibration for 120 extreme events in the catchments of the rivers Danube and Tisza in the period from 2008 to 2013. Although there are limitations when applying the method to extreme events, we found the calibration to be useful for the case of the extreme floods that occurred in May and June 2013 along the Danube.

Comparing model and observed climates

ECMWF has regularly provided ensemble re-forecasts since March 2008 (Hagedorn, 2008; Gneiting, 2014). Ensemble re-forecasts are generated by using the current model version to produce forecasts for previous years within a time window starting on the current date. Today 11-member 46-day re-forecasts are operationally generated for the last 20 years every Monday and Thursday. In the period investigated (2008–2013), five-member re-forecasts were available once a week (on Thursdays).

Ensemble calibration (Box A) can bring valuable improvements if there is a significant difference between the probability distributions of model and observed climates (Ihász et al., 2010). Significance was investigated with two-sample Kolmogorov-Smirnov tests. A stable

Calibration method

A

Calibration is the statistical adjustment of a forecast to improve its quality. In the approach presented here, to perform a calibration the following data are needed, averaged over each river catchment area:

- Model climate: the model climate cumulative distribution function (CDF) derived from re-forecasts.
- Observed climate: the CDF derived from observed data.
- Ensemble forecast: the CDF of the current ENS forecast.

To calibrate the ensemble forecast, it was adjusted by the difference between the observed climate and the model climate. A greater difference between the climates requires a greater adjustment of the ensemble forecast. If the observed climate and the model climate are close, the required adjustment is small.

It is important for all climate CDFs to cover the same period of time. If the period under consideration is too short, it may not include any extreme events. The result of the calibration is an adjusted ENS CDF. Forecasters can compare this with the uncalibrated, raw CDF to help them decide whether or not to adjust the precipitation forecast.

model climate can be produced by using re-forecasts from five consecutive weeks centred on the current date. A model climate was produced for each week of every year in the selected period (2008–2013).

Differences between the probability distributions of model and observed climates are liable to change as a result of changes to the model (Figure 1). For example, the horizontal resolution of ENS was 50 km between 2006 and 2010 and 32 km (up to day 10) between 2010 and 2016. The vertical resolution was 62 levels between 2006 and 2013 and it has been 91 since 2013.

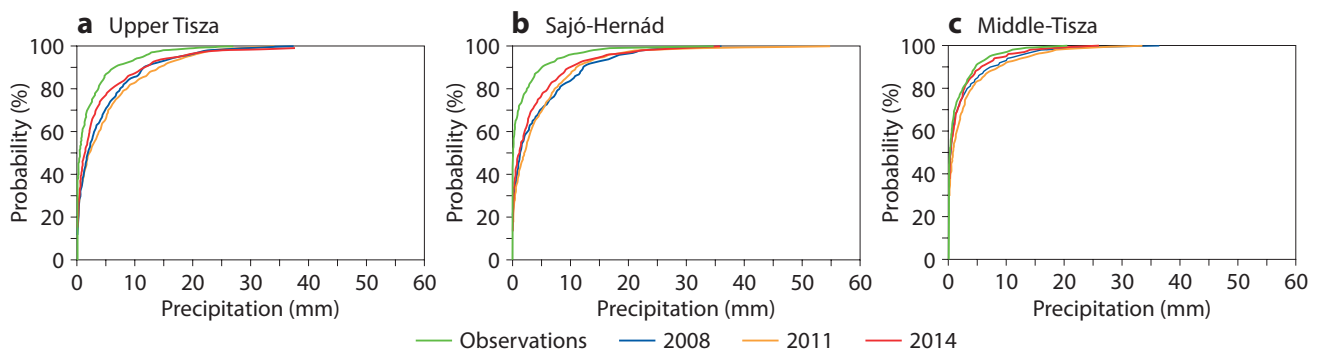


Figure 1 Cumulative distribution functions for 20-year model climates for 24-hour precipitation based on 78-hour re-forecasts over a five-week period centred on the end of May, using ECMWF model versions operational in 2008, 2011 and 2014, and for the observed climate for (a) a mountainous catchment area (Upper-Tisza), (b) a mixed catchment area (Sajó-Hernád), and (c) a flat catchment area (Middle-Tisza). The cumulative distribution functions show the probability that the amount of 24-hour precipitation will not exceed a given threshold.

To investigate the differences between model and observed climates, we compared the observed climate with consecutive model climates for 20 individual catchment areas of the Danube and Tisza rivers. The catchments were divided into three catchment types: flat, mountainous and mixed. Model climates for different years were also compared to capture the impact of changes to the model.

The following general conclusions can be drawn:

- There tend to be considerable differences among the model climates for the same catchment depending on the model version used.
- The model climates based on the model versions operational in 2011 and 2008 are closer to each other than those based on 2014 and 2011.
- The differences between the model and observed climates are relatively small for small to moderate amounts of precipitation in flat regions. As a result, there is generally no need for calibration in these cases. This is especially true for the 2014 model climate.
- In the case of mountainous or mixed catchments and generally in the case of heavy or extreme precipitation, the differences are larger, so calibration is beneficial.
- The smallest differences between the model climate and the observed climate can be seen in the climate based on the model version operational in 2014.

Seasonal and annual similarities and differences were examined by applying the Kolmogorov-Smirnov test to model climates. Model climates based on the model versions operational in 2008 and 2014 were considered in order to capture the influence of model developments. A similar investigation was carried out for the observed and the 2014 model climate to discern the strengths and weaknesses of the model and to support decision-making in situations when there is a risk of flooding. Results show that larger differences usually appear in summer due to more intense convection. The largest differences between the model and observed climates for 2014 appear in spring and summer. The largest differences between model climates (2008 and 2014) were found in summer. This highlights the positive impact of model development on convective precipitation forecasts.

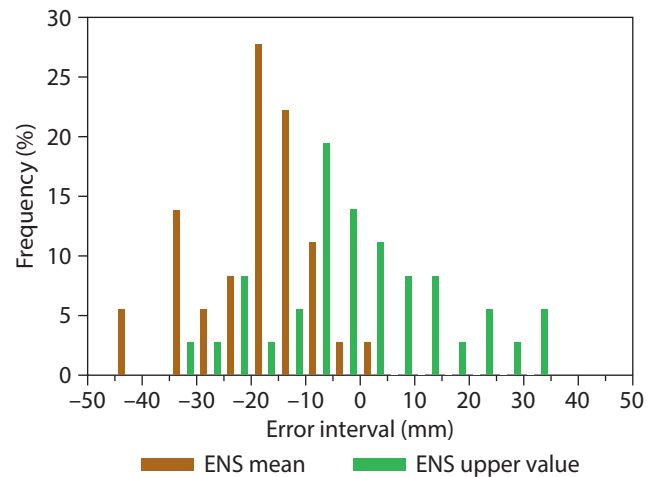


Figure 2 Error distribution of uncalibrated ensemble forecasts of 24-hour precipitation 30 to 54 hours ahead, for 120 cases of extreme precipitation in the period from 2008 to 2013. The chart shows the frequency in per cent for the ensemble mean (brown) and for the ensemble member predicting the largest amount of precipitation (green).

Verification of 120 extreme events

Figure 2 shows the error distribution of uncalibrated ensemble forecasts for 120 extreme 24-hour precipitation events in the upper Danube area in the period from 2008 to 2013. It can be seen that the ensemble mean tends to underestimate the amount of precipitation in these cases. The ENS member predicting the largest amount of precipitation under- and over-estimates the observed precipitation amount in approximately the same proportion.

For the verification of ENS forecasts the Talagrand diagram is widely used. This type of diagram shows how often observations match different parts of an ensemble forecast distribution. To this end, the ensemble forecast distribution is divided into bins of equal size by ensemble member number, for example going from low predicted amounts of precipitation to high predicted amounts of precipitation. In a reliable ensemble forecast, the frequency of observations in each bin will be the same as each part of the ensemble forecast distribution is equally likely.

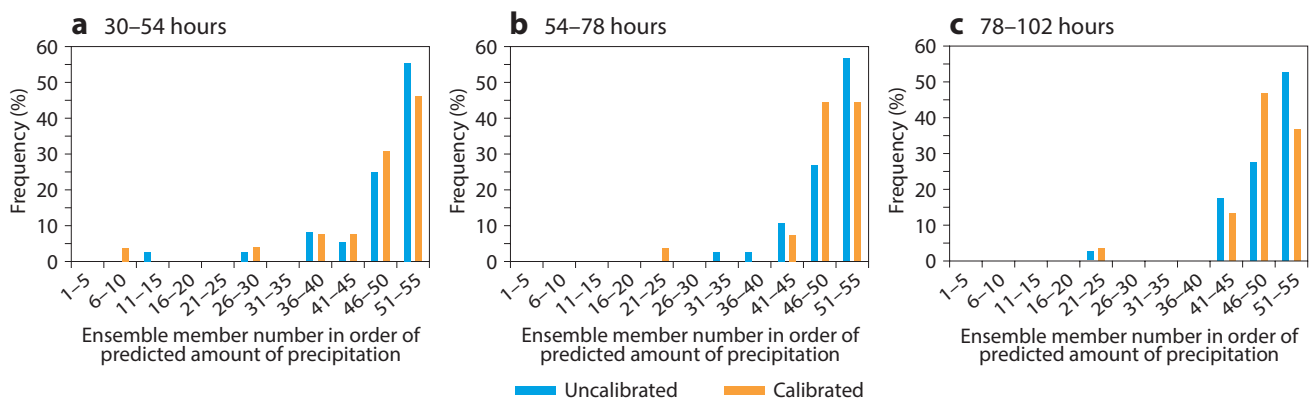


Figure 3 Talagrand diagrams for calibrated and uncalibrated ensemble forecasts of 24-hour precipitation for 120 cases of extreme precipitation in the period from 2008 to 2013, for lead times of (a) 30 to 54 hours, (b) 54 to 78 hours and (c) 78 to 102 hours

Figure 3 shows such diagrams for uncalibrated and calibrated ensemble forecasts and different lead times for 120 cases of extreme precipitation in the upper Danube area in the period from 2008 to 2013. The distribution is slightly more even in the case of calibrated forecasts, which means that extreme events are less likely to be outliers in the ensemble forecast distribution. The calibration method thus improved forecasts of extreme precipitation.

Danube flood May–June 2013

In late May and early June 2013, due to intense cyclonic activity over a few days in the area of the Alps, a severe flood event caused massive damage in the upper Danube region. In Hungary the water level exceeded the previous record level reached in 2002 in most parts of the river except the southern part, near the Hungarian-Serbian border. The flooding was caused by extreme precipitation that fell over the course of four days in the three upper catchments of the Danube. The largest amount of daily precipitation was recorded on 2 June 2013: an average amount of 34.6 mm/24 h in the upper Danube region,

48.2 mm/24 h in the Inn region, and 53.1 mm/24 h in the Traun-Enns region.

Figure 4 shows ECMWF’s 90-hour high-resolution forecast (HRES) and ensemble forecast (ENS) of 24-hour precipitation starting at 12 UTC on 30 May 2013. It can be seen that the area of intense precipitation was well predicted. However, the HRES over-predicted and the ENS mean under-predicted the daily precipitation amount by about 10–20 mm throughout the period. It is important to note that the position and the intensity of the extreme event were well predicted by both HRES and ENS several days ahead.

Figure 5 shows an ENS 12-hour precipitation plume and HRES 12-hour precipitation forecast for the upper Danube area starting at 00 UTC on 29 May 2013. The forecast predicts intense precipitation between days 2 and 5, and this is when heavy rain was indeed observed. The ENS prediction comes with a large spread and the ENS mean is much lower than the HRES on day 4. However, the ENS spread decreased in subsequent, shorter-term forecasts.

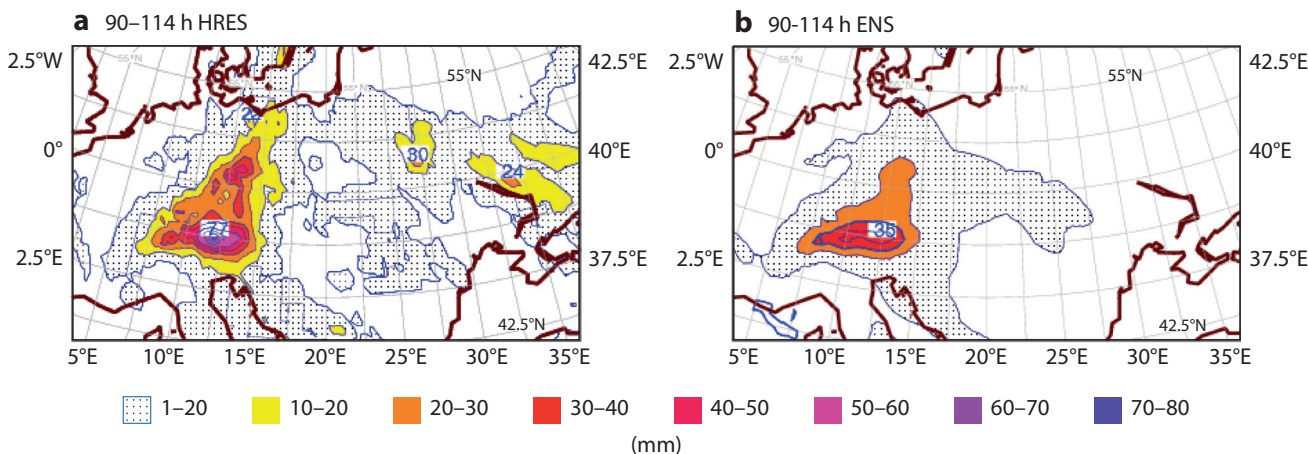


Figure 4 Precipitation forecasts starting at 12 UTC on 30 May 2013 showing (a) the HRES 24-hour precipitation forecast 90 to 114 hours ahead and (b) the ENS mean 24-hour precipitation forecast 90 to 114 hours ahead.

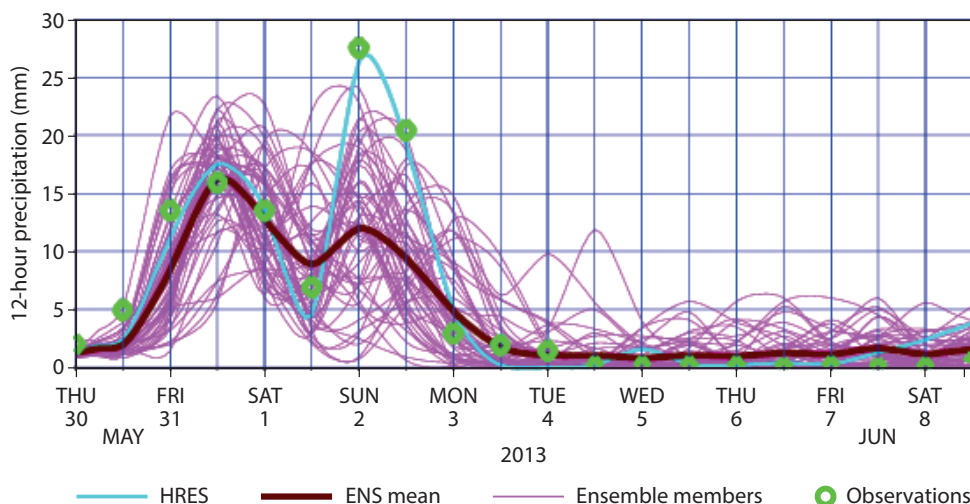


Figure 5 ENS 12-hour precipitation plume and HRES forecast for the upper Danube area starting at 12 UTC on 29 May 2013.

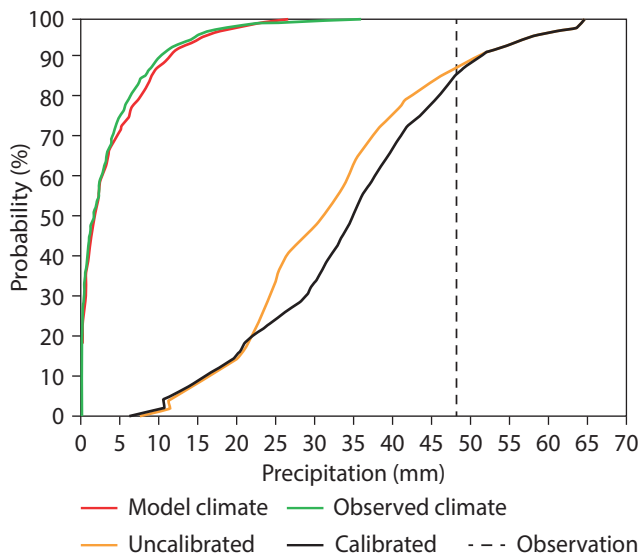


Figure 6 Calibrated and uncalibrated two-day 24-hour precipitation forecasts starting at 00 UTC on 31 May 2013 for the Inn area, shown together with the observed climate and the model climate for that area at that time of year. The vertical dashed line shows the observed value.

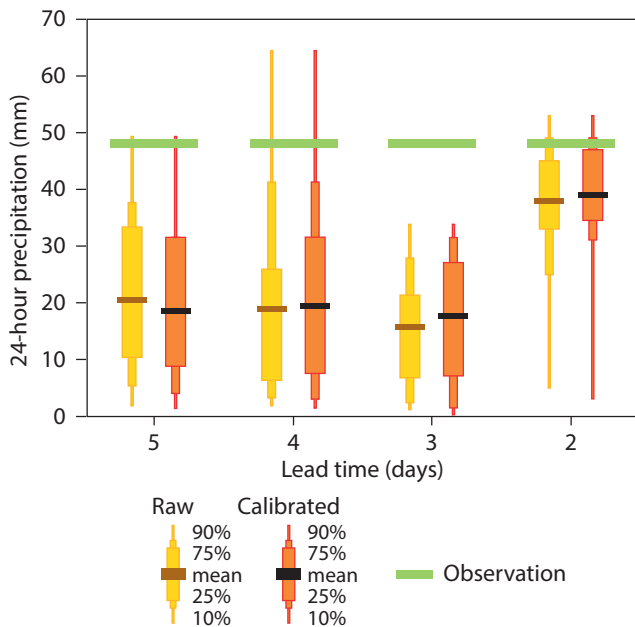


Figure 7 Calibrated and uncalibrated 24-hour precipitation forecasts valid for 06 UTC 1 June 2013 – 06 UTC 2 June 2013 for the Inn catchment area, initialised on four consecutive days starting from 06 UTC on 27 May. The horizontal line shows the observed value.

Figure 6 shows the effect of calibrating the two-day ENS for 24-hour precipitation in the Inn area starting from 00 UTC on 31 May 2013. In this case the observed climate and the model climate are fairly close together. For precipitation amounts up to about 22 mm, the model climate tends to be wetter than the observed climate, while beyond 22 mm it is drier. As a result, the calibration adjusts the ensemble forecast, which predicts a high probability of precipitation above 22 mm, towards even higher probabilities for large amounts of precipitation. However, there is no difference between the calibrated and the uncalibrated forecast beyond 50 mm because of a lack of re-forecast and observational data in that range.

Figure 7 shows how calibrated forecasts are shifted slightly towards higher precipitation values compared to uncalibrated ones in 4, 3 and 2-day forecasts of 24-hour precipitation in the Inn area valid for 06 UTC 1 June to 06 UTC 2 June 2013. It can be seen that the calibration moves the forecast slightly towards the observed value of 48.2 mm. Comparing the raw forecast with the calibrated forecast, forecasters can decide whether or not they need to modify the predicted amount of precipitation.

Summary

We have shown that ensemble precipitation forecasts can be improved using the calibration technique presented here. The observed and model climates were easy to produce from observational data and ECMWF re-forecasts. The model climate should be compared with the observed climate in each river catchment area separately because the differences in the climates can depend on differences in terrain. In our investigation we used regional averages in the calibration. However, in principle it would be better to apply the calibration to individual grid points since the forecasting model uses grid point data.

FURTHER READING

- Gneiting, T.**, 2014: Calibration of medium-range weather forecasts. *ECMWF Technical Memorandum No. 719*.
- Hagedorn R.**, 2008: Using the ECMWF reforecast dataset to calibrate EPS forecasts, *ECMWF Newsletter No. 117*, 8–12.
- Ihász, I., Z. Üveges, M. Mile & Cs. Németh**, 2010: Ensemble calibration of ECMWF’s medium-range forecasts. *Időjárás*, **114**, 275–286.

The new ECMWF interpolation package MIR

**PEDRO MACIEL, TIAGO QUINTINO,
UMBERTO MODIGLIANI, PAUL DANDO,
BAUDOUIIN RAOULT, WILLEM DECONINCK,
FLORIAN RATHGEBER, CRISTIAN SIMARRO**

To use ECMWF forecasts, users typically need to either transform the data from its original spherical harmonics representation (spectral space) into grid space (physical space) or map the data from the model's Gaussian grid to a grid adapted to their needs. These operations are mostly carried out in user requests to the ECMWF real-time product generation system, to the MARS archiving and retrieval system, or within tools such as Metview and the ECMWF Web API.

The interpolation software used until now to perform these transformations, which is part of the EMOSLIB package, has progressively outgrown its original design and implementation limitations. As a result, it has become hard to extend and maintain. ECMWF is about to replace it with the new Meteorological Interpolation and Regridding (MIR) software package developed in-house. The primary goal of MIR is to replace the current EMOSLIB interpolation functions. Beyond this, MIR's flexible design facilitates scalability improvements and additional features. These include efficiency gains, a high degree of user configurability, and support for a wider range of grids than in the current package.

MIR design

The EMOSLIB interpolation package was written in the 1980s and much has changed since then: the model grid resolution has steadily increased, a variety of grid types have been introduced (Malardel et al., 2016), and many new parameters have been added over the years, often associated with different processing requirements. Both software and hardware technologies, such as programming languages, design paradigms, supporting libraries and hardware architectures, have evolved significantly. Together with new numerical methods and ECMWF's improved understanding of user requirements, all these aspects have prompted ECMWF to design the new, extensible and easy-to-maintain MIR package.

MIR features configurable operations and comes with reasonable defaults; it can be extended and configured by users; and it uses Atlas, ECMWF's framework for the development of efficient numerical weather prediction (NWP) and climate applications, to implement its data structures and numerical techniques. Compute-intensive numerical operations are delegated to a linear algebra interface with backend libraries able to provide specialised support for GPUs, accelerator cards and other specific hardware.

MIR builds on past experience and is aligned with the new possibilities enabled by advances in high-performance computing. Ideas and code contributions from multiple teams at ECMWF are continuously improving the different

code bases. MIR uses the spectral transforms library in the Integrated Forecasting System (IFS), the Atlas, ecKit and MARS libraries, and well established standard libraries (FFTW, Eigen) and their hardware or vendor-specific optimised implementations (array operations, GPU, multi-core, etc.). Building on well-defined interfaces and consistent behaviour, the development effort is being shared and re-used across different projects, and MIR's functionality is provided downstream to a wide range of the Centre's services.

Under the hood

MIR is implemented in C++, a programming language appropriate for expressing object-oriented (OO) designs. C++ is also suitable for high-performance computing (HPC) and portable to different hardware architectures. The right balance of language features, such as dynamic polymorphism (inheritance) and static polymorphism (including generic programming), helps to keep the code

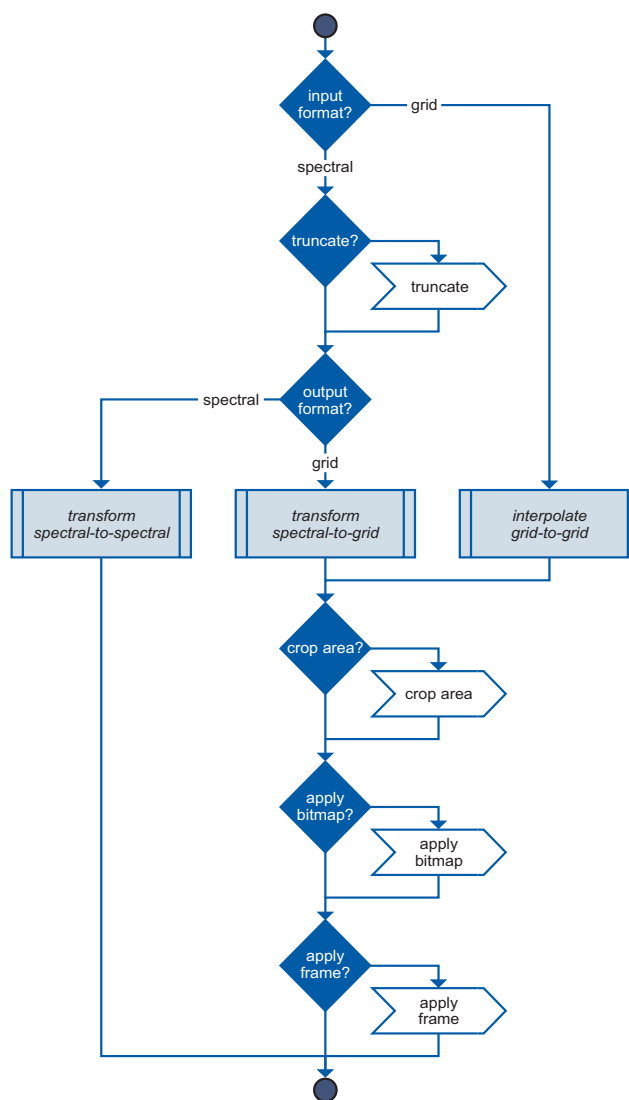


Figure 1 This example flowchart shows how a MIR action plan is prepared.

very concise, readable and extensible. All this makes the code easy to maintain.

Through the MIR API, users (or client software) define an interpolation task by providing both the description of the required interpolation, such as the characteristics of the target grid and the method to use, and the source fields to interpolate from. Together with a third aspect, the default interpolation settings, MIR prepares an ‘action plan’ to execute the request in order to provide the user with the desired result. The fundamental concept in MIR is the data processing pipeline. It is composed of interpolation operators to process input data with deferred execution. The preparation of the action plan involves decisions on which actions to use and how they are parametrized. The

preparation of the action plan can be specific to a ‘style’, of which two are being tested: ‘MARS’ and ‘Dissemination’. These styles mimic the respective operational services and implement their characteristics whilst ensuring consistent results across the services.

Figure 1 shows an example flowchart for the preparation of the action plan, effectively a data processing pipeline. Such flowcharts can be interpreted as directed acyclic graphs (DAG). In an environment that processes requests in parallel, such as product generation, processing pipelines are combined to construct a data processing tree (arborescence), exemplified in Figure 2. Operations have to match in both type and parametrization to be merged. This approach effectively minimises the

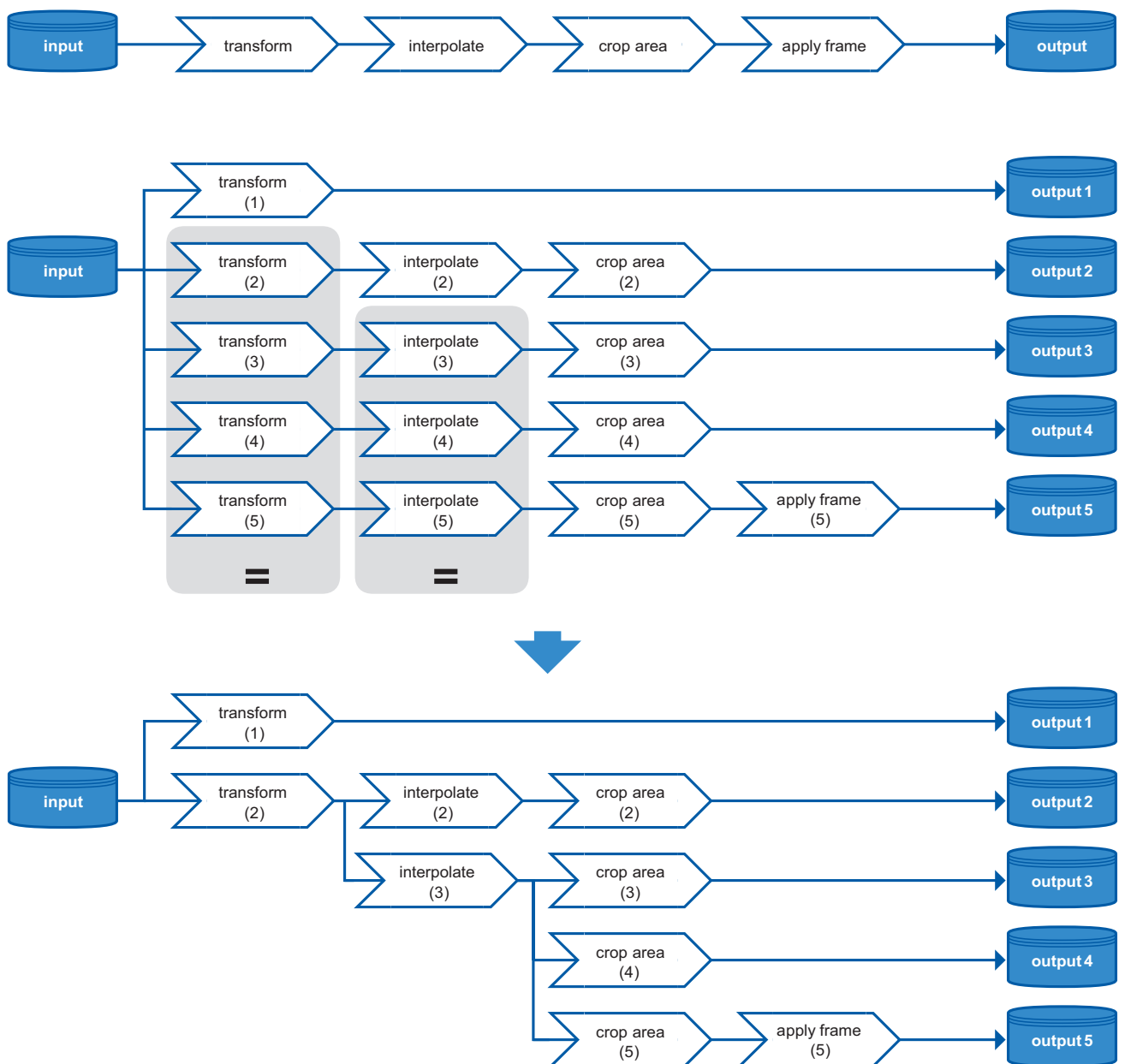


Figure 2 Two types of processing pipelines (action plans): a serial execution pipeline (top) and two parallel execution processing trees (middle and bottom). The middle pipeline has identically parametrized operations, identified by numbers, which are merged into single operations in the bottom pipeline, thus streamlining the process.

number of total operations and thus runtime and input/output (I/O).

The most performance-critical of these operations are additionally supported by caching mechanisms, which enables performance gains for repeated operations. Caching not only expedites the usual spectral transform coefficients calculation but also the calculation of the matrix used in grid-to-grid interpolations and area crop mappings. Actions range from interpolations (grid-to-grid), transformations (spherical harmonics to grid space) and corrections (adjusting wind direction) to generic post-processing (such as truncation, area cropping or bitmapping). Each action is applied to input data whose output acts as input to the next action in the plan. Actions are described in an OO logical and extensible hierarchy. The two most relevant interpolation action classes are described below.

Grid-to-grid interpolation

Actions of this class interpolate between two grids using a ‘method’. The method is responsible for assembling a linear system matrix (say **W**) which relates the input data vector (field data **a**) to the output data vector **b = Wa**. The matrix entries can be corrected for missing values, the presence of a land sea mask or other shape preserving corrections.

The linear system abstraction makes it possible to easily vary the method. For instance, a mass conserving method can be expressed in the same system: **b = M_B W M_A a**. The matrices **M_A** and **M_B** are independent of the construction of **W** and relate the surface meshes built from the input and output grids (respectively) to each other. Another example is the support for circular quantities (such as angles or directions) expressed in the Cartesian components of the input and output vectors **[b_x b_y] = W [a_x a_y]**, providing

the Cartesian de- and re-compositions **[a_x a_y] = f(a)** and **b = f⁻¹ ([b_x b_y])**.

The typical interpolation case uses a Finite Element (FE)-based method: each matrix row represents an output point projected from the Earth’s centre to intersect a 3D input surface mesh element (similar to a ray tracing technique). From this intersection the input point interpolation weights are obtained, and hence the equation for the output point. Interpolating in 3D space employs the Earth-Centred, Earth-Fixed (ECEF) coordinate system, which avoids two-dimensional coordinate system singularities and planar projection distortions and is the natural representation of the physical space.

The FE family of methods includes bilinear and linear interpolations, which differ in the supporting mesh element (quadrilaterals and triangles, respectively). Since this general approach operates on spherical surface meshes, it is important to consider the most adequate surface element which will drive the interpolation weights calculation. In the case of linear interpolations, the natural choice for supporting triangle elements is the Lagrange linear shape function, and for quadrilaterals the bilinear interpolation. Both interpolate linearly within the element, and these two options are mapped to the ‘linear’ and ‘bilinear’ methods, respectively. The octahedral reduced Gaussian grid currently used in the IFS has a very suitable structure for triangular tessellation as it is constructed from a hierarchical triangulation of a regular octahedron.

Another typical interpolation case is the ‘k-nearest neighbours’ method, with a configurable choice of *k* neighbours. A common choice is to use the ‘nearest neighbour’ method (*k* = 1). To retrieve each output point’s neighbours, a supporting *k*-dimensional tree structure makes the search very efficient. Consistent with the FE family of methods described above, the 3D distance of the output point to these neighbour input points is used to determine the interpolation weights and thus to build the matrix used in the linear system.

Since FE-based interpolation methods are driven by the elements composing the mesh, the methods are not necessarily confined to structured meshes. Unstructured meshes can be built for point clouds using Atlas and interpolated to and from other structured or unstructured meshes. In a different way, the *k*-nearest neighbours methods also naturally support arbitrary point clouds because they are not mesh-based. Other methods can be conceived, for example, exploiting the structured nature of the grid for significant speed gains and lower memory requirements. The implementation of these numerical techniques – interpolation methods and mesh generation – is supported by Atlas. Figure 3 shows a remapping from a temperature field point cloud and associated unstructured mesh to a regular grid. Figure 4 shows a geopotential height field remapped from high resolution TCo1279 (HRES operational ‘cubic-octahedral’ grid) to a very coarse TCo31.

Spherical harmonics to grid space

The spectral transform which converts a field between

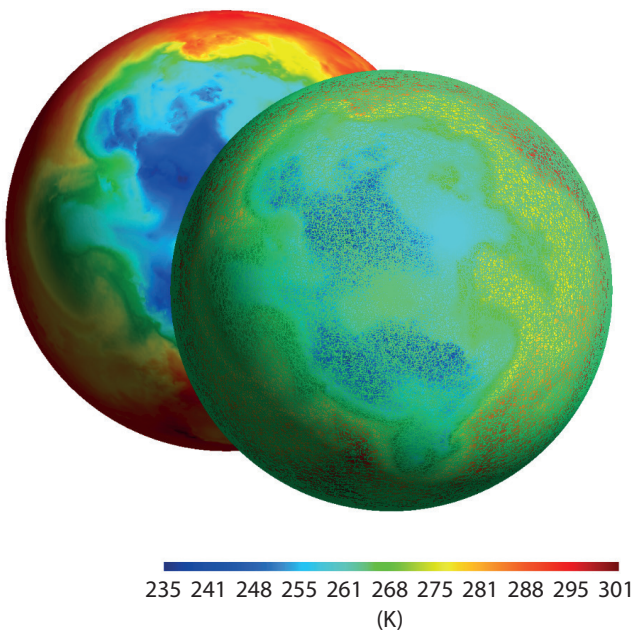


Figure 3 Upper atmosphere temperature field in grid space (back) interpolated from a point cloud (an arbitrary set of data points not following a structure) and associated unstructured mesh (front). MIR can perform transformations from one into the other.

spectral space and grid space is handled by Trans (the spectral transforms library in the IFS). It combines the Fourier and Legendre transforms when going from physical to spectral space (forward transform) and the inverse Legendre and inverse Fourier transforms when going from spectral to physical space (backward transform). The latter direction is the one chiefly of interest for MIR.

MIR uses Trans to transform data from spectral space to grid space: scalar fields and wind vorticity/divergence are transformed into Cartesian components. It also uses Trans to convert vorticity/divergence into Cartesian components within spectral space. All these operations share the implementation used in the IFS. Recent improvements in Trans introduced the more computationally efficient fast Legendre transform (FLT), from which MIR also benefits.

Spectral transformations are computationally very expensive. MIR includes a caching mechanism to handle the pre-calculated coefficients that speed up successive calculations, after the initial transform coefficient calculation. This mechanism can handle cache files both on disk and in memory. The user is also given control of these operations by defining the truncation (if any is required) to apply to the coefficients. MIR always defaults to a truncation choice that is consistent with the grid resolution of the operational data.

Validation

To substitute the current operational functionality based on EMOSLIB, a thorough validation of MIR results started in late 2016 and is scheduled to finish later this year. There are several aspects to the validation, ranging from the data the IFS handles and data from product generation to data in the MARS archive. There are also many additional sources of data included in the validation, such as HRES/ENS, ERA projects, Copernicus, etc. To efficiently test the variety of data handled for post-processing, four parameter interpolation classes have been planned:

- Upper atmosphere parameters, testing the correctness of spectral truncations and transforms; this includes transforms of scalar parameters, such as temperature or geopotential height, and of wind vorticity/divergence to Cartesian components (vector)
- Wave model parameters, testing the correct handling of special grid formats, application of directional interpolations, non-interpolation of spectra and associated parameters, and correctness near the coast
- Surface parameters, testing a relevant sample of surface parameters and associated specialised treatments, such as the role of land–sea masks and parameter-specific corrections
- Special cases such as precipitation threshold, sub-area handling, Copernicus new parameters, shifted grids, simulated satellite images, etc.

A validation suite, which encompasses a large and growing set of tests, has been created to cover the testing sections above. A substantial amount of testing has already been carried out and the first two parameter interpolation classes in the list above are very close to completion. Testing has so far identified issues in both MIR and the current operational interpolation software.



Figure 4 Surface geopotential height field (in $\text{m}^2 \text{s}^{-2}$) interpolated from an octahedral reduced Gaussian grid TCo1279 (HRES operational grid, back) to low resolution TCo31 (front). The colour palette is qualitative, for illustrative purposes only.

As a result, it has been possible to improve the quality of both. In addition, using the validation suite will increase confidence when making any changes to MIR in the future.

The validation process is following a very agile process: much of the testing suite runs in parallel and on different platforms. Testing is usually carried out within one of the classes above, or it is restricted to a specific grid type or parameter. When an issue is identified, such as a significant difference when compared against reference results, it is submitted to the issue-tracking system.

What will change for users?

The aim is to replace the existing operational interpolation software in all its uses. Most users interact with the interpolation package through their MARS requests and Metview macros, or indirectly with product generation requests, and in these cases the changes for users will be minimal.

With the new interpolation closely linked to the IFS's Atlas library, it is ensured that ECMWF software and operational services can react fast to new research developments. This will be especially important in the coming years when testing innovative grids and numerical methods.

Test versions of MIR will be made available to all users later this year. The first operational use of MIR as part of the MARS client and product generation system used at ECMWF is expected for next year. After that a new API will be developed and released. MIR's flexible design will allow the addition of extra features, such as additional interpolation features, e.g. mass conservation.

FURTHER READING

Malardel, S., N. Wedi, W. Deconinck, M. Diamantakis, C. Kühnlein, G. Mozdzyński, M. Hamrud & P. Smolarkiewicz, 2016: A new grid for the IFS, *ECMWF Newsletter No. 146*, 23–28.

ECMWF Calendar 2017/18

Sep 11–14	Annual Seminar – Ensemble prediction: past, present and future
Oct 2–5	Training course: Use and Interpretation of ECMWF Products
Oct 9–11	Scientific Advisory Committee
Oct 12–13	Technical Advisory Committee
Oct 16	Policy Advisory Committee
Oct 17–18	Finance Committee
Nov 3	Advisory Committee of Co-operating States
Nov 13–16	Workshop on shedding light on the greyzone
Nov 13–17	5th International Conference on Reanalysis (ICR5) (Rome)
Dec 4–6	ECMWF/ESA Workshop on Using Low-Frequency Passive Microwave Measurements in Research and Operational Applications
Dec 7–8	Council
Jan 22–25	Workshop on observations and analysis of sea-surface temperature and sea ice for NWP and climate applications
Jan 22–26	Training course: ecFlow
Jan 29 – Feb 2	Training course: Use and interpretation of ECMWF products
Feb 5–9	Training course: Use and interpretation of ECMWF products
Feb 19–22	Training course: ecCodes, BUFR
Feb 26 – Mar 01	Training course: ecCodes, GRIB

Mar 12–16	NWP training course: Data assimilation
Mar 19–23	EUMETSAT/ECMWF NWP-SAF training course: Satellite data assimilation
Apr 9–13	Advisory Committee for Data Policy and data policy meetings of EUMETSAT and ECOMET
Apr 16–20	NWP training course: Advanced numerical methods for Earth system modelling
Apr 23–27	NWP training course: Parametrization of subgrid physical processes
Apr 24	Policy Advisory Committee
Apr 25–26	Finance Committee
Apr 30 – May 4	NWP training course: Predictability and ensemble forecast systems
Jun 4–7	Using ECMWF's Forecasts (UEF)
Jun 13–14	Council
Sep 10–13	Annual Seminar
Sep 24–28	Workshop on high-performance computing in meteorology
Oct 1–3	Training course: Use and interpretation of ECMWF products
Oct 8–10	Scientific Advisory Committee
Oct 11–12	Technical Advisory Committee
Oct 22–23	Finance Committee
Oct 24	Policy Advisory Committee
Dec 4–5	Council

ECMWF publications

(see <http://www.ecmwf.int/en/research/publications>)

Technical Memoranda

- 805 **Xiao, H., M. Diamantakis & S. Saarinen:** An OpenACC GPU adaptation of the IFS cloud microphysics scheme. *June 2017*
- 803 **Tietsche, S., M.A. Balmaseda, H. Zuo & P. de Rosnay:** Comparing Arctic winter sea-ice thickness from SMOS and ORAS5. *June 2017*
- 802 **Chambon, P. & A.J. Geer:** All-sky assimilation of Megha-Tropiques/SAPHIR radiances in the ECMWF numerical weather prediction system. *June 2017*
- 801 **Bozzo, A., S. Remy, A. Benedetti, J. Flemming, P. Bechtold, M.J. Rodwell & J.J. Morcrette:** Implementation of a CAMS-based aerosol climatology in the IFS. *April 2017*

- 800 **Bonavita, M., Y. Trémolet, E. Holm, S.T.K. Lang, M. Chrust, M. Janiskova, P. Lopez, P. Laloyaux, P. de Rosnay, M. Fisher, M. Hamrud & S. English:** A Strategy for Data Assimilation. *April 2017*
- 799 **Lean, P., A. Geer & K. Lonitz:** Assimilation of Global Precipitation Mission (GPM) Microwave Imager (GMI) in all-sky conditions. *April 2017*
- 798 **Lawrence, H., F. Carminati, W. Bell, N. Bormann, S. Newman, N. Atkinson, A. Geer, S. Migliorini, Q. Lu & K. Chen:** An evaluation of FY-3C MWRI and Assessment of the long-term quality of FY-3C MWHS-2 at ECMWF and the Met Office. *April 2017*

Index of Newsletter articles

This is a selection of articles published in the *ECMWF Newsletter* series during recent years.

Articles are arranged in date order within each subject category.

Articles can be accessed on ECMWF's public website – <http://www.ecmwf.int/en/research/publications>

	No.	Date	Page		No.	Date	Page
NEWS							
ECMWF supports flood disaster response in Peru	152	Summer 2017	2	Experts debate future of supercomputing in meteorology	150	Winter 2016/17	13
New data centre to be located in Bologna	152	Summer 2017	4	Météo-France hosts OpenIFS workshop	149	Autumn 2016	2
New Director of Research takes up his post	152	Summer 2017	4	Predicting heavy rainfall in China	149	Autumn 2016	4
Ten years of forecasting atmospheric composition at ECMWF	152	Summer 2017	5	ECMWF makes S2S forecast charts available	149	Autumn 2016	5
OpenIFS used by University of Reading students	152	Summer 2017	6	Graduate trainees enjoyed their time at ECMWF	149	Autumn 2016	6
EFAS and GloFAS seasonal hydrological outlooks	152	Summer 2017	7	Copernicus Climate Change Service tracks record global temperatures	149	Autumn 2016	7
Flood forecast decision-making games	152	Summer 2017	9	Experts discuss role of drag processes in NWP and climate models	149	Autumn 2016	8
ECMWF meets its users: UEF 2017	152	Summer 2017	10	ECMWF hosts Year of Polar Prediction meeting	149	Autumn 2016	9
Record numbers attend ECMWF's NWP courses	152	Summer 2017	12	ECMWF releases software for observational data	149	Autumn 2016	10
ECMWF air quality data competition has a winner	152	Summer 2017	13	Survey shows MARS users broadly satisfied	149	Autumn 2016	11
A fresh look at tropical cyclone intensity estimates	152	Summer 2017	14	Supercomputing project reviews performance analysis tools	149	Autumn 2016	12
ECMWF helps to upgrade Sri Lankan forecasting capability	152	Summer 2017	16	ANYWHERE and IMPREX hold general assemblies	149	Autumn 2016	13
End of the road for GRIB-API	152	Summer 2017	16	New Strategy is "ambitious but not unrealistic"	148	Summer 2016	2
New IFS version control and issue tracking tools	152	Summer 2017	17	Forecasts showed Paris flood risk well in advance	148	Summer 2016	4
The cold spell in eastern Europe in January 2017	151	Spring 2017	2	Better temperature forecasts along the Norwegian coast	148	Summer 2016	6
ECMWF launches eLearning	151	Spring 2017	4	Atmospheric composition forecasts move to higher resolution	148	Summer 2016	7
New layers in updated ecCharts service	151	Spring 2017	6	OBE for Alan Thorpe	148	Summer 2016	7
ECMWF–CMEMS agreement on sea-level anomaly data	151	Spring 2017	7	New satellite data reduce forecast errors	148	Summer 2016	8
Forecast performance 2016	151	Spring 2017	8	ECMWF steps up assimilation of aircraft weather data	148	Summer 2016	10
Complex supercomputer upgrade completed	151	Spring 2017	10	GloFAS meeting supports integrated flood forecasting	148	Summer 2016	11
Open data in the spotlight during week of events	151	Spring 2017	11	First Scalability Day charts way forward	148	Summer 2016	13
Devastating wildfires in Chile in January 2017	151	Spring 2017	12	Evaluating forecasts tops agenda at 2016 user meeting	148	Summer 2016	14
Copernicus fire danger forecast goes online	151	Spring 2017	14	First Women in Science Lunch held at ECMWF	148	Summer 2016	15
Talks with Italy on new data centre under way	151	Spring 2017	15	New Director of Forecasts appointed	148	Summer 2016	16
ECMWF joins OpenWIS Association	151	Spring 2017	15	Croatian flag raised at ECMWF	148	Summer 2016	16
ECMWF installs electric vehicle charging points	151	Spring 2017	15	Web standards for easy access to big data	148	Summer 2016	17
Flash floods over Greece in early September 2016	150	Winter 2016/17	2	Joint work with CMA leads to second S2S database	148	Summer 2016	18
ECMWF widens role in WMO severe weather projects	150	Winter 2016/17	4	ECMWF takes part in WMO data monitoring project	148	Summer 2016	19
New opportunities from HEO satellites	150	Winter 2016/17	5				
Lakes in weather prediction: a moving target	150	Winter 2016/17	6	VIEWPOINT			
New Director of Research appointed	150	Winter 2016/17	7	Living with the butterfly effect: a seamless view of predictability	145	Autumn 2015	18
New Council President elected	150	Winter 2016/17	7	Decisions, decisions...!	141	Autumn 2014	12
ERA5 aids in forecast performance monitoring	150	Winter 2016/17	8	Using ECMWF's Forecasts: a forum to discuss the use of ECMWF data and products	136	Summer 2013	12
ECMWF to work with RIMES on flood forecasting	150	Winter 2016/17	8	Describing ECMWF's forecasts and forecasting system	133	Autumn 2012	11
Scientists discuss methods to simulate all-scale geophysical flows	150	Winter 2016/17	9				
C3S trials seasonal forecast service	150	Winter 2016/17	10				
Multi-decadal variability in predictive skill of the winter NAO	150	Winter 2016/17	11				
ECMWF meets Ibero-American weather services	150	Winter 2016/17	12				

	No.	Date	Page		No.	Date	Page
COMPUTING							
The new ECMWF interpolation package MIR	152	Summer 2017	36	New model cycle brings higher resolution	147	Spring 2016	14
Climate service develops user-friendly data store	151	Spring 2017	22	Reducing systematic errors in cold-air outbreaks	146	Winter 2015/16	17
ECMWF's new data decoding software ecCodes	146	Winter 2015/16	35	A new grid for the IFS	146	Winter 2015/16	23
Supercomputing at ECMWF	143	Spring 2015	32	An all-scale, finite-volume module for the IFS	145	Autumn 2015	24
SAPP: a new scalable acquisition and pre-processing system at ECMWF	140	Summer 2014	37	Reducing surface temperature errors at coastlines	145	Autumn 2015	30
Metview's new user interface	140	Summer 2014	42	Atmospheric composition in ECMWF's Integrated Forecasting System	143	Spring 2015	20
GPU based interactive 3D visualization of ECMWF ensemble forecasts	138	Winter 2013/14	34	Towards predicting high-impact freezing rain events	141	Autumn 2014	15
				Improving ECMWF forecasts of sudden stratospheric warmings	141	Autumn 2014	30
				Improving the representation of stable boundary layers	138	Winter 2013/14	24
				Interactive lakes in the Integrated Forecasting System	137	Autumn 2013	30
				Effective spectral resolution of ECMWF atmospheric forecast models	137	Autumn 2013	19
METEOROLOGY				PROBABILISTIC FORECASTING & MARINE ASPECTS			
OBSERVATIONS & ASSIMILATION							
Assessing the impact of observations using observation-minus-forecast residuals	152	Summer 2017	27	Monitoring thin sea ice in the Arctic	152	Summer 2017	23
CERA-20C: An Earth system approach to climate reanalysis	150	Winter 2016/17	25	The 2015/2016 El Niño and beyond	151	Spring 2017	16
The use of radar altimeter products at ECMWF	149	Autumn 2016	14	Twenty-one years of wave forecast verification	150	Winter 2016/17	31
Joint project trials new way to exploit satellite retrievals	149	Autumn 2016	20	Hungary's use of ECMWF ensemble boundary conditions	148	Summer 2016	24
Global radiosonde network under pressure	149	Autumn 2016	25	What conditions led to the Draupner freak wave?	148	Summer 2016	37
Use of forecast departures in verification against observations	149	Autumn 2016	30	Using ensemble data assimilation to diagnose flow-dependent forecast reliability	146	Winter 2015/16	29
Use of high-density observations in precipitation verification	147	Spring 2016	20	Have ECMWF monthly forecasts been improving?	138	Winter 2013/14	18
GEOOWOW project boosts access to Earth observation data	145	Autumn 2015	35				
CERA: A coupled data assimilation system for climate reanalysis	144	Summer 2015	15	METEOROLOGICAL APPLICATIONS & STUDIES			
Promising results in hybrid data assimilation tests	144	Summer 2015	33	Calibrating forecasts of heavy precipitation in river catchments	152	Summer 2017	32
Snow data assimilation at ECMWF	143	Spring 2015	26	Reanalysis sheds light on 1916 avalanche disaster 'L'alluvione di Firenze del 1966': an ensemble-based re-forecasting study	148	Summer 2016	31
Assimilation of cloud radar and lidar observations towards EarthCARE	142	Winter 2014/15	17	Diagnosing model performance in the tropics	147	Spring 2016	26
The direct assimilation of principal components of IASI spectra	142	Winter 2014/15	23	NWP-driven fire danger forecasting for Copernicus	147	Spring 2016	34
Automatic checking of observations at ECMWF	140	Summer 2014	21	Improvements in IFS forecasts of heavy precipitation	144	Summer 2015	21
All-sky assimilation of microwave humidity sounders	140	Summer 2014	25	New EFI parameters for forecasting severe convection	144	Summer 2015	27
Climate reanalysis	139	Spring 2014	15	The skill of ECMWF cloudiness forecasts	143	Spring 2015	14
Ten years of ENVISAT data at ECMWF	138	Winter 2013/14	13	Calibration of ECMWF forecasts	142	Winter 2014/15	12
Impact of the Metop satellites in the ECMWF system	137	Autumn 2013	9	Twenty-five years of IFS/ARPEGE	141	Autumn 2014	22
Ocean Reanalyses Intercomparison Project (ORA-IP)	137	Autumn 2013	11	Potential to use seasonal climate forecasts to plan malaria intervention strategies in Africa	140	Summer 2014	15
The expected NWP impact of Aeolus wind observations	137	Autumn 2013	23	Predictability of the cold drops based on ECMWF's forecasts over Europe	140	Summer 2014	32
Winds of change in the use of Atmospheric Motion Vectors in the ECMWF system	136	Summer 2013	23	Windstorms in northwest Europe in late 2013	139	Spring 2014	22
				Statistical evaluation of ECMWF extreme wind forecasts	139	Spring 2014	29
FORECAST MODEL							
IFS Cycle 43r3 brings model and assimilation updates	152	Summer 2017	18	Flow-dependent verification of the ECMWF ensemble over the Euro-Atlantic sector	139	Spring 2014	34
New IFS cycle brings sea-ice coupling and higher ocean resolution	150	Winter 2016/17	14	iCOLT – Seasonal forecasts of crop irrigation needs at ARPA-SIMC	138	Winter 2013/14	30
Impact of orographic drag on forecast skill	150	Winter 2016/17	18	Forecast performance 2013	137	Autumn 2013	13
Single-precision IFS	148	Summer 2016	20				

Contact information

ECMWF, Shinfield Park, Reading, Berkshire RG2 9AX, UK

Telephone National 0118 949 9000

Telephone International +44 118 949 9000

Fax +44 118 986 9450

ECMWF's public website <http://www.ecmwf.int/>

E-mail: The e-mail address of an individual at the Centre is firstinitial.lastname@ecmwf.int. For double-barrelled names use a hyphen (e.g. j-n.name-name@ecmwf.int).

Problems, queries and advice	Contact
General problems, fault reporting, web access and service queries	servicedesk@ecmwf.int
Advice on the usage of computing and archiving services	advisory@ecmwf.int
Queries regarding access to data	data.services@ecmwf.int
Queries regarding the installation of ECMWF software packages	software.support@ecmwf.int
Queries or feedback regarding the forecast products	forecast_user@ecmwf.int



Newsletter | Number 152 – Summer 2017
European Centre for Medium-Range Weather Forecasts
www.ecmwf.int